

RESEARCH PAPER

Cold tolerance of woodland strawberry (*Fragaria vesca*) is linked to Cold Box Factor 4 and the dehydrin Xero2

Adnan Kanbar¹, Christoph Hubertus Weinert², , David Kottutz¹, La Thinh¹, Eman Abuslima^{1,3}, Farida Kabil⁴, Mohamed Hazman^{5,6}, Björn Egert², Bernhard Trierweiler², Sabine Emma Kulling², and Peter Nick^{1,*}, 

¹ Molecular Cell Biology, Joseph Köreuter Institute for Plant Sciences, Karlsruhe Institute of Technology, Fritz-Haber-Weg 4, D-76131 Karlsruhe, Germany

² Max Rubner-Institut, Federal Research Institute of Nutrition and Food, Department of Safety and Quality of Fruit and Vegetables, Haid-und-Neu-Straße 9, D-76131 Karlsruhe, Germany

³ Department of Botany and Microbiology, Faculty of Science, Suez Canal University, Ismailia 41522, Egypt

⁴ Vegetable Crops Department, Faculty of Agriculture, Cairo University, Giza, Egypt

⁵ Agricultural Genetic Engineering Research Institute (AGERI), Agricultural Research Center (ARC), 9 Gamma-Street, Giza-12619, Egypt

⁶ School of Biotechnology, Nile University, Juhayna Square, 26th of July Corridor, El Sheikh Zayed, Giza, Egypt

* Correspondence: peter.nick@kit.edu

Received 10 November 2023; Editorial decision 10 May 2024; Accepted 17 July 2024

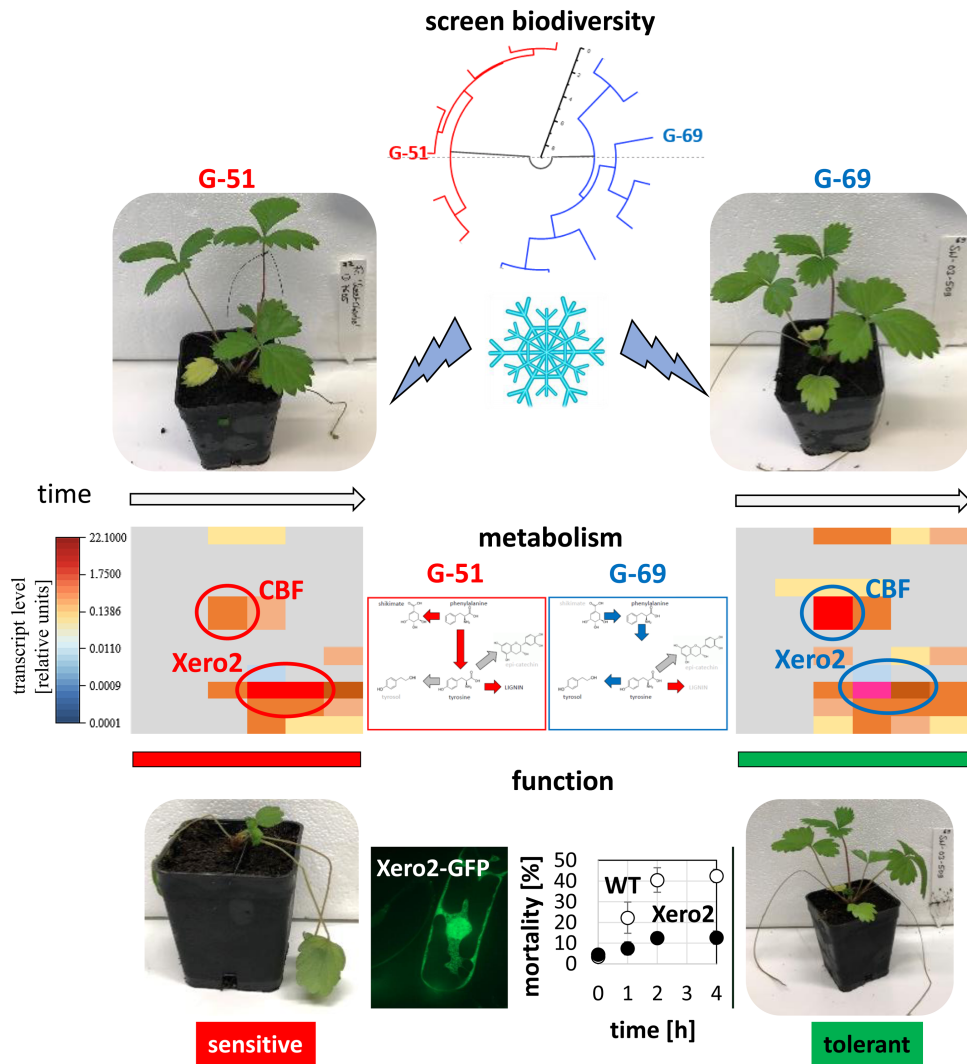
Editor: Fabrizio Costa, University of Trento, Italy

Abstract

Domesticated strawberry is susceptible to sudden frost episodes, limiting the productivity of this cash crop in regions where they are grown during early spring. In contrast, the ancestral woodland strawberry (*Fragaria vesca*) has successfully colonized many habitats of the Northern Hemisphere. Thus, this species seems to harbour genetic factors promoting cold tolerance. Screening a germplasm established in the frame of the German Gene Bank for Crop Wild Relatives, we identified, among 70 wild accessions, a pair with contrasting cold tolerance. By following the physiological, biochemical, molecular, and metabolic responses of this contrasting pair, we identified the transcription factor Cold Box Factor 4 and the dehydrin Xero2 as molecular markers associated with superior tolerance to cold stress. Overexpression of green fluorescent protein fusions with Xero2 in tobacco BY-2 cells conferred cold tolerance to these recipient cells. A detailed analysis of the metabolome for the two contrasting genotypes allows the definition of metabolic signatures correlated with cold tolerance versus cold stress. This work provides a proof-of-concept for the value of crop wild relatives as genetic resources to identify genetic factors suitable to increase the stress resilience of crop plants.

Abbreviations: CAT, catalase; CBF, Cold Box Factor; COR gene, cold response gene; CWR, crop wild relative; GABA, γ -aminobutyric acid; GC \times GC-MS, two-dimensional GC-MS; MDA, malondialdehyde; ROS, reactive oxygen species; SOD, superoxide dismutase; WEL, genbank für Wildpflanzen mit Nutzungspotential für Ernährung und Landwirtschaft (gene bank for crop wild relatives).

Graphical abstract



Keywords: Cold Box Factor 4, cold stress, crop wild relative, *Fragaria vesca*, metabolomics, woodland strawberry.

Introduction

Cold stress represents a facet of global climate change that is often neglected. Due to evolutionary adaptation, plants in temperate regions have adjusted their development to the seasonal temperature pattern. Cold periods are bridged by reduced metabolic activity controlled by abscisic acid. In spring, the dissipation of abscisic acid releases the block, allowing growth and development to continue. This metabolic relaunch comes at a price, namely a sharp drop in cold resistance. For instance, bud-break in grapevine is accompanied by strongly decreased frost tolerance (Fuller and Telli, 2008). Blurred seasonality as a consequence of global climate change uncouples the evolutionary adaptation of plant development from ambient temperature,

simply because temperature fluctuations become progressively erratic. This is illustrated by a dendrochronological study in Illinois showing very clearly how the risk for spring damage has increased over the last century (Augsburger, 2013). Likewise, climate modelling predicts that global warming, while reducing the frequency of extreme cold snaps, will not reduce their intensity and duration (Kodra *et al.*, 2011). This means that episodes of cold stress occurring out of synchrony with plant development will be even more demanding for the agriculture of the 21st century.

These considerations highlight that a deeper understanding of cold adaptation is crucial to prepare agriculture for the

challenges of global climate change. The quality of cold stress strongly depends on temperature, genotype, and their mutual interaction. Especially in subtropical or tropical plants, chilling is already sufficient to cause severe damage, a phenomenon for which [Molisch \(1897\)](#) coined the term *Erkältung*. Chilling sensitivity is often linked to specific stages in the life cycle—for instance, flowering in rice cannot occur when the night temperature drops below 18 °C, and the fruit of cucumber rot rapidly when experiencing a cold snap of <10 °C. Cold stress is one of the major reasons why certain crops do not occur in temperate regions (see [Lyons, 1973](#) for a comprehensive review). While chilling is linked with metabolic imbalance and therefore may be reversible to a certain extent, freezing injury caused by subzero temperatures is irreversible, and can be lethal as intracellular ice crystals damage membranes, disrupting the integrity of the cell. Interestingly, many plants can cope with freezing when they have been hardened off by chilling. This adaptive response is called cold acclimation or cold hardening (a classical review is given in [Guy, 1990](#)).

Low temperature is a physical signal in the first place. The primary input is a drop in membrane fluidity which needs to be converted into a chemical signal to deploy a cellular response. This conversion (susception) is brought about by cortical microtubules adjacent to the membrane that will collect and amplify the minute mechanical forces caused by membrane rigidification (for a review on the role of microtubules in cold susception, see [Wang et al., 2020](#)). As a result, calcium influx is deployed. In rice, which is very chilling sensitive, calcium influx is facilitated by activation of the transmembrane protein COLD1, a regulator of the plant trimeric G-protein RGA ([Ma et al., 2015](#)). However, the extent to which this plays a role in freezing-tolerant species other than rice is questionable. In addition to calcium influx, oxidative burst via a membrane-located NADPH oxidase is a necessary element of early transduction ([Wang and Nick, 2017](#)). Early signals are transduced into the nucleus through kinase cascades that cross-talk in a complex, partially synergistic, partially antagonistic manner (for a discussion, see [Wang et al., 2020](#)), converging on the accumulation of the master switch Inducer of CBF expression 1 (ICE1; for a review, see [Chinnusamy et al., 2007](#)). Accumulation of ICE1 will then activate the Cold Box Factors (CBFs), transcriptional activators for cold response (COR) genes, leading to cold adaptation (for a recent review, see [Shi et al., 2018](#)).

While most of the CBFs are conserved among different species and overlap functionally, one particular subset, CBF4, is specific. This group of transcription factors is only found in species capable of freezing tolerance. It is induced more slowly than the other CBFs, but persists longer, as found, for instance, in leaves and buds of grapevine ([Xiao et al., 2008](#)). Therefore, CBF4 is thought to be the master switch for cold acclimation. For instance, comparative proteomics with strawberry varieties differing in cold tolerance showed a correlation between the abundance of CBF4 and cold tolerance ([Koehler et al., 2012](#)).

Functional evidence for this hypothesis comes from experiments where constitutive overexpression of *VvCBF4* produced grapevines with superior freezing tolerance ([Tillett et al., 2012](#)). CBF4 also differs in terms of subcellular localization. Unlike the other CBFs, it is not constitutively located in the nucleus but is imported from the perinuclear cytoplasm in response to cold stress ([Shi et al., 2022](#)).

Cold stress has a particular impact on valuable, but highly sensitive cash crops, such as the garden strawberry (*Fragaria × ananassa* Duch.). With a current global production of more than €2500 million per year (<https://www.tridge.com/intelligences/stawberry/EG/production>), strawberries belong to the economically most relevant fruit crops, but are highly sensitive to untimely cold snaps (for a review, see [Tuteja et al., 2012](#)). Production systems specializing in producing this fruit early in the year, ahead of competitors in other countries, are especially vulnerable. Strawberry production in Egypt can be used as a paradigm to illustrate this point. Here, the main production period is the winter season, which makes production especially vulnerable to untimely cold snaps. With a long history starting from the early 19th century, still under the reign of Mohamed Ali ([Arafat, 2019](#)), strawberry cultivation experienced a strong boom from the 1980s, mainly in the Nile Delta. As a consequence, it has become a strong export commodity to the Arab and European markets, with an estimated export volume of 600 000 t, particularly in the season from November to April, when production in many European countries is diminished or limited to greenhouses (<https://www.tridge.com/intelligences/stawberry/EG/production>). Thus, cold resilience would be a favourable trait in garden strawberry.

This also holds true for post-harvest processing. Fruits such as strawberries are often refrigerated for storage and transport to slow down the decay of fruit quality, and thus to extend the period of commercial availability. Under appropriate conditions, well-storable fruit or vegetables can be conserved for several months (apples, [Hatoum et al., 2014](#); pears, [Yi et al., 2020](#); onions, [Romo-Pérez et al., 2020](#); potatoes, [Datir et al., 2020](#)), and even perishable fruits often for at least a few weeks (peaches, [Brizzolara et al., 2018](#); [Wang et al., 2021](#); strawberries, [Lv et al., 2022](#); tomatoes, [Delgado-Vargas et al., 2022](#)). For this reason, research on the physiological and metabolic changes during cold storage has focused mainly on the impact of mid- or long-term exposure to cold, with the aim of extending storage life or to gain a better understanding of post-harvest diseases such as chilling injuries (mangosteen, [Vega-Alvarez et al., 2020](#); tomatoes, [Delgado-Vargas et al., 2022](#); peach, [Wang et al., 2021](#); [Brizzolara et al., 2018](#); strawberry, [Ayala-Zavala et al., 2005](#); [Asghari and Hasanlooe, 2015](#); [Aghdam et al., 2021](#)). However, apart from such traditional storability studies, short-term cooling of fruit is relevant as well, especially with respect to ensuring a high quality of very perishable fruit in the supply chain. For strawberry in particular, rapid cooling very soon after harvest is crucial for reducing post-harvest losses ([do Nascimento Nunes et al., 1995](#); [Neuwald et al., 2021](#)).

Domestication has selected for traits linked to fast development, such as suppression of dormancy or stimulation of growth, and for high yield, including suppressed seed shed or increased fruit size (Abbo *et al.*, 2014). This has come at the expense of resilience since allocation of resources for growth competes with those available for resilience. By providing optimal conditions including fertilization, irrigation, suppression of weeds, and plant protection against pathogens, humans compensated for this, such that the loss of resilience did not lead to reduced fitness under the conditions of domestication. Climate change is challenging this symbiotic interaction between *Homo sapiens* and his crops, shifting crop wild relatives (CWRs) into the focus, since they provide gene pools for resilience factors. In many crops, these factors can be valorized by introgression into high-yielding crop varieties. In polyploid crops such as strawberry or potato, where introgression is difficult, knowledge of these resilience factors would at least help to identify promising genotypes or design genome-editing strategies. In the past, the use of resilience factors from CWRs was mainly targeted to pathogen resistance (for a review, see Hajjar and Hodgkin, 2007). However, meanwhile, resilience to climate change has acquired renewed attention (for a recent review, see Cortés and López-Hernández, 2021). Unfortunately, CWRs are often endangered and, so far, have remained under-represented in the usual germplasm collections. To address this drawback, the German Ministry of Food and Agriculture Germany has established a Gene Bank for Wild Plants with Potential for Nutrition and Agriculture (WEL), comprising ~4000 accessions from ~300 species that had been collected all over the country (Borgmann *et al.*, 2014). While this germplasm reflects only a minute fraction of the wild populations of these species, it was sampled over different climatic zones and

ecosystems, and thus might be considered a pragmatic approximation to biodiversity.

In search of genetic factors contributing to cold resilience, we screened accessions for woodland strawberry (*F. vesca* L.) from the WEL gene bank. These accessions originated from elevated locations with harsher climatic conditions. In fact, we detected a considerable genetic variation with respect to cold tolerance. By screening 70 wild accessions collected in 13 sites, we defined a pair of contrasting genotypes that were then characterized for their physiological, biochemical, molecular, and metabolic responses. As the metabolic responses of strawberry fruit to short-term cold stress ('chilling') have not been studied in sufficient detail so far, we addressed this issue in the current study in addition to using metabolomics.

Materials and methods

Plant materials

The study used 13 field samples comprising 70 individuals of woodland strawberry (*F. vesca* L.) collected in South Germany during the years 2010–2018 as part of the project Genbank für Wildpflanzen mit Nutzungspotential für Ernährung und Landwirtschaft (Gene Bank for Wild Plants with Potential Use for Nutrition and Agriculture) by the German Federal Ministry of Food and Agriculture. In addition, one accession of green strawberry (*F. viridis* Weston) and one accession of Chilean strawberry [*F. chiloensis* (L.) Mill], one of the ancestral species of the garden strawberry, were included. For both of these accessions, the Nagoya protocol does not apply, since they entered the garden before 2014, the year when Germany signed the protocol. Achenes of all accessions are maintained at $-20\text{ }^{\circ}\text{C}$ in the WEL Genebank Southwest (Botanical Garden, Karlsruhe Institute of Technology) and in the Central WEL Germplasm Repository (Botanical Garden, Osnabrück University). Details of accession numbers, collection sites, year of collection, and cold tolerance are given in Table 1. The seeds were placed in vacuum-sealed bags and stored

Table 1. List of the 16 wild strawberry accessions analysed, with their respective genotype ID, voucher number of the KIT Botanical Garden (now JKIP Experimental Station), name of the species, place and year of collection, and mean score of leaf wilting

Genotype Number	Genotype ID	Species	Place of collection	Year of collection	Leaf wilting score
G-4	KIT 7223	<i>F. chiloensis</i>	Kykeon Plants	2010	9
G-8	WEL SW-05-431	<i>F. vesca</i>	Reutlingen Mittlere Kuppenalb	2013	5
G-35	WEL SO-01-0208	<i>F. vesca</i>	Bayern; Schwandorf Falkensteiner Vorwald	2013	5
G-38	WEL SO-01-0034	<i>F. vesca</i>	Bayern; Neumarkt i. d. OPf. Mittlere Frankenalb	2010	1
G-68	WEL SW-03-502	<i>F. vesca</i>	Rhein-Neckar-Kreis Bergstrasse	2013	1
G-69	WEL SW-03-509	<i>F. vesca</i>	Schwarzwald-Baar-Kreis Südöstlicher Schwarzwald	2013	1
G-49	WEL SW-05-398	<i>F. vesca</i>	Zollernalbkreis Hohe Schwabenalb	2013	5
G-26	WEL SW-03-217	<i>F. vesca</i>	Rastatt Nördlicher Talschwarzwald	2011	7
G-29	WEL SW-03-508	<i>F. vesca</i>	Freudenstadt Mittlerer Schwarzwald	2013	7
G-32	WEL SO-01-1031	<i>F. vesca</i>	Bayern; Berchtesgadener Land Berchtesgadener Alpen	2013	7
G-39	WEL SO-01-0649	<i>F. vesca</i>	Bayern; Neumarkt i. d. OPf. Südliche Frankenalb	2012	5
G-40	WEL SO-01-0653	<i>F. vesca</i>	Bayern; Regensburg Südliche Frankenalb	2012	5
G-47	WEL SO-01-0253	<i>F. vesca</i>	Bayern; Berchtesgadener Land Berchtesgadener Alpen	2011	7
G-51	WEL SW-05-447	<i>F. vesca</i>	Sigmaringen Baaralb und Oberes Donautal	2013	7
G-60	KIT 6184	<i>F. viridis</i>	Botanical Garden Iasi (Romania)	2011	9

WEL, Genbank für Wildpflanzen mit Nutzungspotential für Ernährung und Landwirtschaft, German Federal Ministry of Nutrition and Agriculture; KIT, Karlsruhe Institute of Technology. Leaf wilting score was taken after cold treatment ($-6\text{ }^{\circ}\text{C}$) for 6 h.

at $-20\text{ }^{\circ}\text{C}$ till use. Clonal material for screening was generated by a two-step protocol. The achenes of the 15 accessions were raised to generate 70 plantlets that were treated as separate genotypes, since woodland strawberry shows a high degree of outcrossing (Irkaeva and Ankudinova, 1994) such that the achenes of a given accession are genetically heterogenous. These 70 individuals were then clonally propagated to obtain genetically homogenous offspring for the screening. Surface-sterilized achenes were sown into 5 litre plastic pots filled with a mixture of one volume each of peat moss, perlite, and soil, and raised in the greenhouse at $22 \pm 3\text{ }^{\circ}\text{C}$ with a 12 h photoperiod. Each pot contained one plant. Irrigation was performed to maintain 80% of field capacity. Mean relative humidity for crop growing periods was $\sim 70\%$, ranging from 65% to 75%. Daylight was supplemented by a sodium incandescent light (SON-T AGRO, Philips, 400W/220 E40 55000 lm) fixed at 3 m above the plants to maintain an intensity of $\sim 1000\text{ }\mu\text{mol m}^{-2}\text{ s}^{-1}$ photosynthetically active radiation (PAR) at noon. A continuous flow of fresh air was maintained during the entire experimental period to ensure sufficient supply of CO_2 . After runners had developed, they were separated from their mother and raised in the same manner. This vegetative propagation was repeated over four generations to generate sufficient clonal material from each of the 70 progenitor plants.

Screening for cold tolerance

Since cold tolerance derives from chilling and freezing tolerance as components that are not necessarily coupled, we carried out screening under different conditions. First, all genotypes were screened for chilling tolerance: three clonal daughters per genotype with 5–7 leaves were transferred to 0.5 litre plastic pots filled with a mixture of a 1:1:1 peat moss:perlite:soil mixture and incubated in a climate chamber ($22 \pm 3\text{ }^{\circ}\text{C}$, $120\text{ }\mu\text{mol m}^{-2}\text{ s}^{-1}$ PAR, 70% humidity, and a cycle of 12 h light and 12 h dark) for 10 d for pre-adaptation to the new soil. Then, three leaves from each plant were selected and photographed to document their status prior to the stress treatment. Subsequently, the cold treatment was initiated by reducing the temperature in the growth chamber to $+5\text{ }^{\circ}\text{C}$ for 12 h in the dark and $+11\text{ }^{\circ}\text{C}$ for 12 h in light, while maintaining light intensity and relative humidity. Plants were irrigated once daily to maintain 80% of field capacity. After 21 d of chilling stress, the three leaves were photographed again. To assess the degree of damage, leaf area and decoloration were determined by quantitative image analysis (ImageJ, <https://imagej.nih.gov/ij/>) according to Wang *et al.* (2019). Since exploratory experiments had shown that all genotypes were endowed with a relatively high level of chilling tolerance, we redesigned the screen with a higher stringency, again with three plants of each genotype and a developmental stage with 5–7 leaves. Now, we simulated freezing stress of a frosty night by transferring the plantlets into a freezing chamber and exposing them to $-6\text{ }^{\circ}\text{C}$ for 6 h in darkness, allowing the response to develop for 1 h after the end of the freezing treatment. To evaluate the response, we assessed leaf wilting using a non-parametrical ranking system with a scale of 1–9 (1=no wilting, 3=few leaves showed wilting, 5=half of the leaves showed wilting, 7=severe wilting, ~ 60 – 80% of the leaves showed wilting, and 9=severely wilted, $>80\%$ of the leaves showed wilting). Representative images for the scoring are given in Supplementary Table S1. To reach sufficient resolution of the different scores and reduce ambiguities of assessment, the even-numbered intermediates of the classes were not used.

Biochemical assays

The biochemical responses were investigated for the cold-tolerant genotype ‘G-69’ and the cold-susceptible genotype ‘G-51’. Clonal plants with 5–7 leaves were transferred from the greenhouse into a climate chamber and kept for 10 d at $22 \pm 3\text{ }^{\circ}\text{C}$ with a 12 h photoperiod for pre-equilibration. Light intensity, relative humidity, and irrigation were as described above. After this pre-equilibration, temperature was decreased to

$+2\text{ }^{\circ}\text{C}$ for the 12 h dark period, and $+7\text{ }^{\circ}\text{C}$ for the 12 h light period, while all other conditions remained unchanged. A control sample was raised in the greenhouse at ~ 20 – $25\text{ }^{\circ}\text{C}$; however, since this experiment was conducted in the summer, at noon temperatures could rise to $28\text{ }^{\circ}\text{C}$. Leaves were sampled for biochemical analysis prior to cold stress (0 h), and at days 7 and 14 after the onset of cold stress in five independent biological repeats:

We measured malondialdehyde (MDA) as the readout for oxidative damage according to Heath and Packer (1968). Leaves were shock-frozen in liquid nitrogen and stored at $-80\text{ }^{\circ}\text{C}$ till analysis. Aliquots of $\sim 100\text{ mg}$ of leaf were ground to a powder with metal beads in a TissueLyzer (Qiagen, Hilden, Germany) and the powder vortexed for 45 s in 1 ml of 0.1 M phosphate buffer (pH 7.4) in a 2.0 ml Eppendorf tube, spun down for 4 min at 8000 g, and then the sediment was discarded. Subsequently, 200 μl of supernatant were added to a reaction mixture containing 750 μl of acetic acid (20% w/v), 750 μl of 2-thiobarbituric acid (aqueous solution, 0.8% w/v), 200 μl of Milli-Q deionized water, and 100 μl of SDS (8.1% w/v). An identical reaction mixture, where the supernatant from the sample was replaced by an equal volume of buffer, was used as a blank. The reaction mixture was incubated at $98\text{ }^{\circ}\text{C}$ for 1 h and then cooled down to room temperature. The absorbance at 535 nm (specific signal) and at 600 nm (background) were recorded by a UV spectrophotometer (Uvicon, Schott, Mainz, Germany), which allows calculation of lipid peroxidation as μM MDA from the ratio of A_{535} over A_{600} using an extinction coefficient of $155\text{ mM}^{-1}\text{ cm}^{-1}$.

Steady-state levels of hydrogen peroxide as readout of oxidative stress were quantified using the method described in Shi *et al.* (2005). The activities of the antioxidant enzymes superoxide dismutase (SOD) and catalase (CAT) were measured according to Beauchamp and Fridovich (1971) and Aebi (1984), respectively. To obtain the specific activities, protein content was determined in the same samples according to Bradford (1976). For these assays, freshly harvested leaf samples ($\sim 500\text{ mg}$ FW) were ground on ice by mortar and pestle in 5 ml of ice-cold potassium phosphate buffer (0.1 M, pH 7.5), liquid extracts centrifuged at 12 000 g for 10 min, at $4\text{ }^{\circ}\text{C}$ (Hermel Z 383 K), and supernatants collected and evaporated to dryness. An aliquot of 100 μl was used to determine protein content according to Bradford (1976). The powder was redissolved in 70% HPLC-grade methanol to a concentration of 10 mg ml^{-1} . The activity of SOD was quantified from the scavenging of light-induced superoxide radicals generated in riboflavin–nitroblue tetrazolium (NBT) according to Beauchamp and Fridovich (1971). The reaction mixture contained 3 ml of 50 mM phosphate buffer (pH 7.6), to which 20 g of riboflavin, 12 mM EDTA, and 0.1 mg of NBT were added in sequence, along with 5 μl of extract. The reaction was started by illuminating the tubes for 2 min at room temperature. Immediately after illumination, the absorbance was measured at 590 nm with a negative control to determine the quantity of formazan produced in the absence of the extract. The percentage of scavenged superoxide anions was calculated from the ratio between A_{590} of the sample and A_{590} of the negative control, which allowed estimation of enzyme activity using an extinction coefficient of $12.8\text{ mM}^{-1}\text{ cm}^{-1}$. The scavenging of hydrogen peroxide as proxy for CAT activity was estimated according to Aebi (1984). Here, different amounts (60–420 μg) of the dried extract were dissolved in 3.4 ml of 0.1 M phosphate buffer (pH 7.4) and mixed with 600 μl of hydrogen peroxide (43 mM), recording A_{230} against butyl-hydroxy-toluol (BHT) as positive control yielding 100% scavenging. The concentration of hydrogen peroxide was then calculated based on an extinction coefficient of $40\text{ mM}^{-1}\text{ cm}^{-1}$. All data on redox parameters are means and standard errors from five biological replicates.

Analysis of gene expression

For gene expression studies, plants were subjected to cold stress ($2\text{ }^{\circ}\text{C}$ during a 12 h dark period, followed by $+7\text{ }^{\circ}\text{C}$ during a 12 h light period) and collected at the indicated time points (from 0 h to 14 d), immediately frozen in liquid nitrogen, and stored at $-80\text{ }^{\circ}\text{C}$ until further

processing. Light intensity, relative humidity, and irrigation were as described above. Total RNA was isolated using the Spectrum™ Plant Total RNA Kit (Sigma, Germany) according to the instructions of the manufacturer from a small amount of tissue (~100 mg FW) after homogenization (Tissue Lyzer, Qiagen, Hilden, Germany) and purified from potential DNA contamination by RNase-free DNase (Qiagen). A template of 1 µg of extracted RNA was reverse transcribed into cDNA by M-MuLV Reverse Transcriptase (New England Biolabs, Frankfurt am Main, Germany) and transcripts of interest were amplified and quantified by real-time quantitative PCR (qPCR) with the CFX96 Touch™ Real-Time PCR Detection System (Bio-Rad Laboratories GmbH, Munich, Germany) using a SYBR Green dye protocol according to [Svyatyna *et al.* \(2014\)](#) and the oligonucleotide primers given in [Supplementary Table S2](#). *Elongation factor 1 alpha (EF1α)* was chosen as an internal standard. The transcript levels were normalized to this standard based on the $2^{-\Delta\Delta C_t}$ method ([Livak and Schmittgen, 2001](#)), using the control value at 0 h for each genotype as a reference, to compare genotypes and transcripts; in some cases, the relative expression based on $2^{-\Delta C_t}$ was also used.

Overexpression of dehydrin Xero2-1 in tobacco BY-2 cells

The dehydrin Xero2-1 (Gene ID: Fv01g101314123) was cloned from G-69 and G-51 and used to construct green fluorescent protein (GFP) fusions making use of the modular GATEWAY® cloning technology for subsequent overexpression in tobacco BY-2 cells. As a control for potential effects of the selection marker or selective stringency by kanamycin, a line was included where GFP was fused to tobacco α -tubulin 3, driven by the same promoter and with the same selective marker and stringency ([Kumagai *et al.*, 2001](#)).

Generation of FvXero2 overexpressor lines in tobacco BY-2

The full-length coding sequence of FvXero2-1 was amplified from the cDNA of both G-69 and G-51 after prolonged cold stress for 7 d as described in ‘Analysis of gene expression’ using a pair of modified primers containing attB sites for recombinant integration into the GATEWAY® donor vector. Initial denaturation was 94 °C for 7 min, followed by 30 cycles of denaturation at 94 °C for 1 min, annealing at 60 °C for 1 min, and elongation at 72 °C for 2 min, terminated by a final elongation step at 72 °C for 4 min. Since the sequences turned out to be identical for the two genotypes, only the amplicon from G-69 was used further. The sequences for the oligonucleotide primers are given in [Supplementary Table S2](#).

The amplicons were first recombined into the entry plasmid pDONR/Zeo (Invitrogen), and then cloned into the binary plasmid pK7WGF2.0 [N-terminal fusion of GFP under control of the constitutive cauliflower mosaic virus (CaMV) 35S promoter, kanamycin resistance], and pK7FWG2.0 (C-terminal fusion of GFP under control of the constitutive CaMV 35S promoter, kanamycin resistance) for stable and transient transformation, respectively. Correct and complete insertion was verified by DNA sequencing (GATC Biotech, Cologne, Germany). The resulting constructs were then used for stable transformations into tobacco BY-2 (*Nicotiana tabacum* L. cv Bright Yellow 2) using a modified *Agrobacterium*-based protocol ([Gao *et al.*, 2016](#)) employing non-transformed BY-2 cells (WT) as control, selecting the transformants by 100 mg l⁻¹ kanamycin. Resistant calli were picked, pooled, and then amplified and used to generate suspension cultures. The cells were cultivated on a weekly rhythm as described by [Schneider *et al.* \(2015\)](#) along with non-transformed tobacco BY-2 cells (WT). To maintain stringency of selection, the cells overexpressing FvXero2-1-GFP were raised under supplementation with 50 mg l⁻¹ kanamycin.

Cold treatment of tobacco BY-2 cells and cell mortality assay

The suspension cells were treated at the peak of mitotic activity, at day 3 after subcultivation. To impose severe cold stress, Erlenmeyer flasks with

the cell suspension were placed in a bath of ice water to maintain a temperature of 0 °C and shaken on an orbital shaker at 100 rpm in darkness for up to 20 h. Aliquots were sampled at specified time points during the cold treatment and scored for cell mortality using the Evans blue dye exclusion assay ([Gaff and Okong’O-Ogola, 1971](#)). Unbound dye was washed out with water three times and then cells were viewed by bright-field microscopy under a AxioImager Z.1 microscope (Zeiss). Data represent means and standard errors from three biological replicates with 500 individual cells scored for each value.

Spinning disc confocal microscopy

The GFP-tagged FvXero2-1 was inspected by spinning disc confocal microscopy (AxioObserver Z1 microscope, Zeiss, Jena, Germany), observing the fluorescence from GFP upon excitation with the 488 nm emission line of an Ar-Kr laser (Zeiss, Jena, Germany). Confocal images were recorded using a Plan Apochromat ×63/1.44 DIC oil objective operated via the Zen 2012 (Blue edition) software platform.

Metabolomics from an outdoor pot experiment

To approximate the situation in the field, and to delineate the metabolic effects of short-term cold stress in leaves and fruit of G-69 and G-51, a total of 20 plants per genotype were cultivated in black 5 litre pots under outdoor conditions in the Botanical Garden of the Karlsruhe Institute of Technology in spring and summer 2020. Information on temperature and rainfall are given in [Supplementary Table S3](#).

Sampling

Since woodland strawberry forms fruits continuously and since the fruits are of small size, the sampling strategy for fruits had to be adapted. Mature fruits (~3 weeks post-anthesis) were collected, pooled from individual plants, and separated into two sets of equal number and comparable weight. One set was subjected to cold stress (2 °C for 6 h in the dark) and the other set was kept for the same period at 25 °C. Directly after the experiment, whole fruit were immersed in liquid nitrogen and afterwards stored at -80 °C until further processing. Leaf sampling was conducted at the end of the harvesting period, on two subsequent days at the beginning of July. The 20 plants were randomized to either the control or the treatment group, such that each group comprised 10 individuals. The control group was sampled immediately, while the treatment group was subjected to cold stress (2 °C) for 6 h, also in the dark, and sampled thereafter. Humidity was 65–70% in both cases. Since the sampling required ~5 min per plant, the plants were transferred to the phytochamber individually in a tiered manner, at intervals of 5 min to ensure a constant duration of the cold stress experiment and to standardize the time frame of the sampling itself. To ensure homogenous development, fully expanded but young leaves were used (plastochron 7–10 on each plant), excising and collecting only the central leaflet. The leaf material was shock-frozen in liquid nitrogen, coarsely ground with a mortar and pestle, transferred to a 50 ml Falcon tube, and stored at -80 °C until further preparation. Both fruit and leaf samples were lyophilized for 72 h (VaCo 5-II D, Zirbus Technology, Bad Grund, Germany) with an ice condenser temperature of -85 °C and at a final pressure of 0.3–0.4 mbar. Afterwards, the samples were ground in a ball mill (model MM400, Retsch, Haan, Germany) with stainless steel cups and beads for 10 s at 25 Hz. Ground samples were again stored at -80 °C in screw-capped tubes.

Untargeted metabolomics

Leaves and fruits from both genotypes were sampled and subjected to untargeted metabolome analysis by one- or two-dimensional gas chromatography-mass spectrometry (GC-MS or GC×GC-MS; Shimadzu) using the parameters given in [Supplementary Table S4](#).

Results

German woodland strawberries comprise cold-susceptible and -tolerant genotypes

To assess the cold responses, all 70 clonal lines deriving from the 13 field isolates for *F. vesca* deposited in the German CWR Gene Bank, along with one accession of *F. viridis* and *F. chiloensis*, respectively (Table 1), were screened for their susceptibility to

chilling stress, evaluating leaf growth and discoloration. In parallel, the same accessions were characterized for their freezing tolerance using a non-parametric wilting index as readout. The phenological data from the 15 progenitor accessions were then subjected to hierarchical cluster analysis (Fig. 1). Five of the *F. vesca* accessions clustered with the highly cold-susceptible *F. viridis* and *F. chiloensis*, while eight of the *F. vesca* accessions formed a different clade with better cold tolerance. Based on this screen,

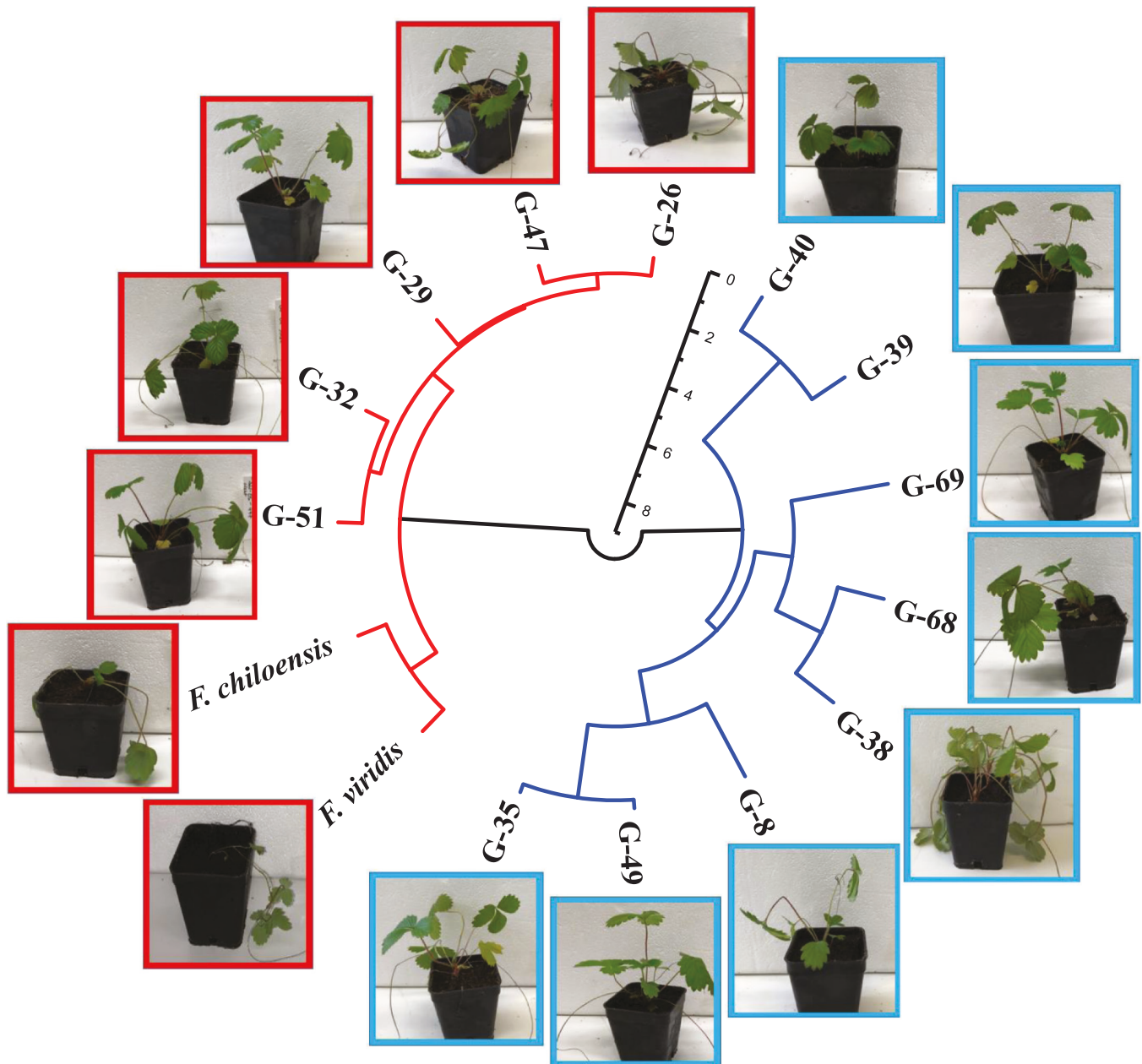


Fig. 1. Hierarchical cluster analysis of the different *F. vesca* genotypes from Germany along with the American *F. chiloensis* and *F. viridis*, based on leaf wilting score, leaf area, and leaf decoloration under cold stress treatment. Leaf area and leaf decoloration were measured before and after 21 d of chilling stress (2 °C for 12 h in the dark and 7 °C for 12 h in light). The wilting score is recorded after 6 h of freezing stress (−6 °C). Dendrogram based on Euclidean distance and Ward's minimum variance method. Data have been Z-score standardized. The blue colour subgroup represents cold-tolerant accessions and the red colour subgroup represents cold-susceptible accessions. Exemplarily genotype G-51 (susceptible) and G-69 (resistant) are shown after freezing stress.

we selected the cold-sensitive G-51 (originating from the Upper Danube valley) and the cold-tolerant G-69 (deriving from the Southeast of the Black Forest) for the subsequent study. While leaves of G-51 had completely lost their turgescence following a freezing episode of $-6\text{ }^{\circ}\text{C}$ for 6 h (Fig. 2, left), the leaves of G-69 were left unharmed by this treatment. Likewise, upon chilling stress, G-69 outperformed G-51, already manifest from day 4 after onset of chilling stress (Fig. 2, centre). Also, the recovery from chilling stress was more efficient in G-69, as evident from a more pronounced fruit set and darker greenish leaves as compared with G-51 (Fig. 2, right).

The cold-tolerant genotype G-69 is endowed with a more robust redox homeostasis

To understand the cold tolerance of G-69, we first monitored redox homeostasis over time in leaves of both genotypes (Fig.

3). Cold stress can perturb electron transport at the thylakoid membrane leading to elevated levels of ROS such as superoxide, resulting in lipid peroxidation culminating in accumulation of the stable end-product MDA. The MDA levels found in the susceptible G-51 were around twice as high as in G-69 (Fig. 3A). SOD, converting superoxide into hydrogen peroxide, was transiently induced with a significantly higher amplitude in G-69, such that activity at day 14 of stress was six times higher than in G-51. The pattern for SOD activity (Fig. 3C) was a mirror image of the pattern seen for MDA levels (Fig. 3A). The hydrogen peroxide resulting from SOD activity can be dissipated further by CAT (Fig. 3D). Again, the specific activity of this enzyme was elevated in G-69 over G-51, albeit not as persistently. The steady-state levels of hydrogen peroxide (Fig. 3B) increased transiently and eased off at a level elevated over that seen before. Here, the two genotypes were similar.

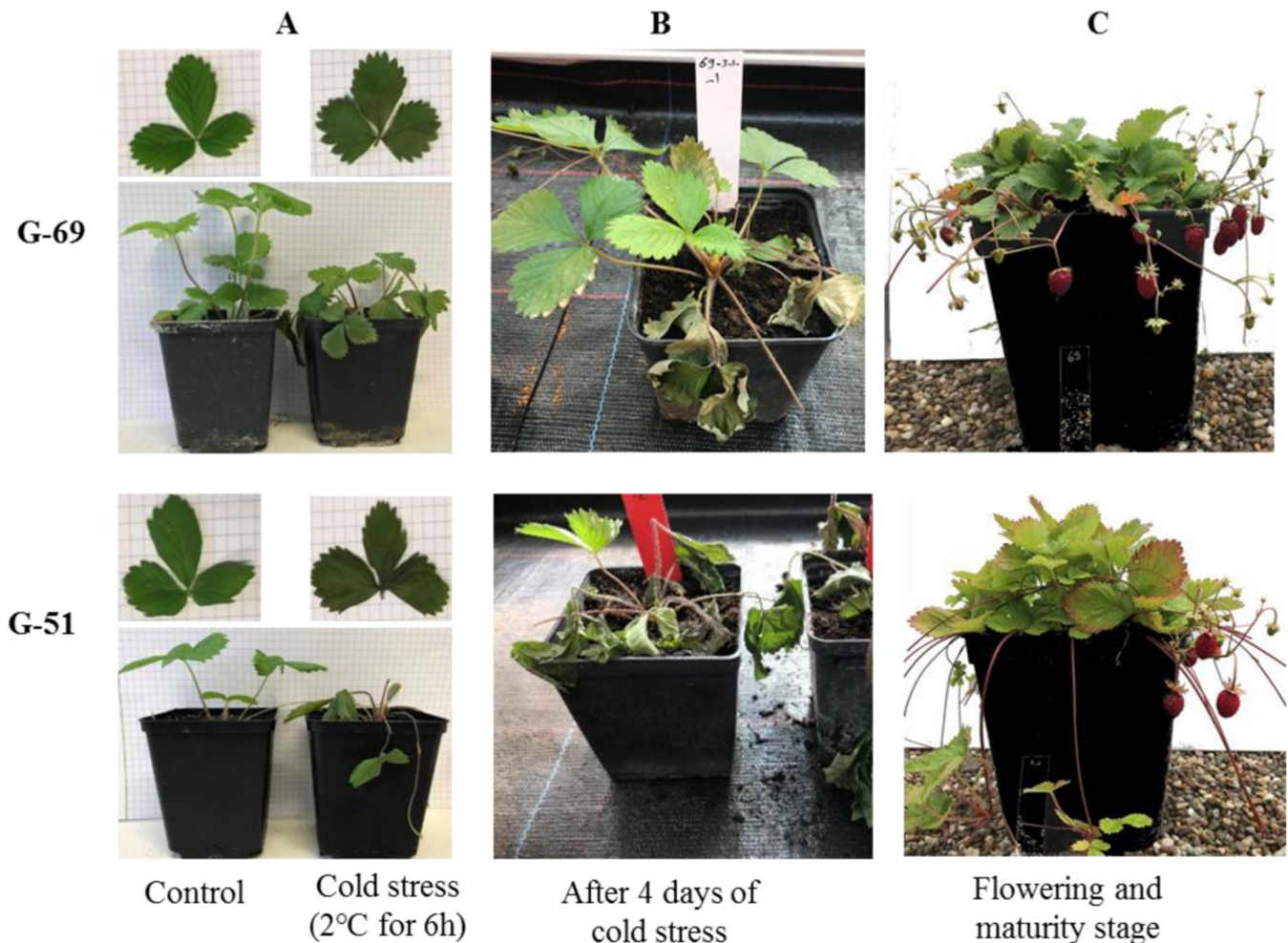


Fig. 2. Representative images illustrating the phenotypic response of a cold-tolerant (G-69) and a cold-susceptible (G-51) genotype of woodland strawberry to freezing stress and subsequent recovery. (A) Plantlets and leaves prior to (left) and following freezing stress (right) at $-6\text{ }^{\circ}\text{C}$ for 6 h. (B) Long-term response to the freezing stress after 4 d of recovery without cold stress. (C) Phenotype at flowering and fruit set.

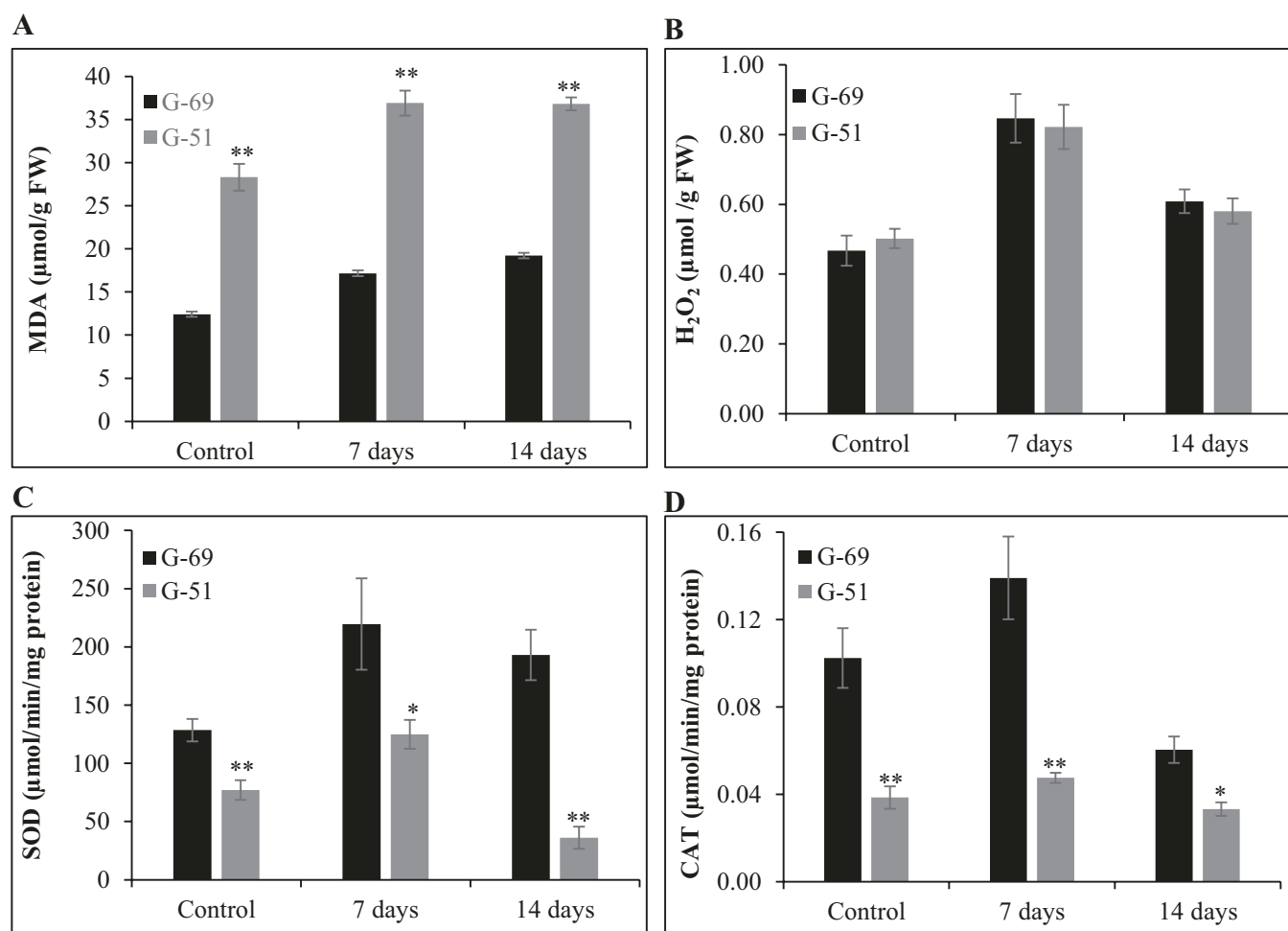


Fig. 3. Effect of cold stress on redox homeostasis. (A) Malondialdehyde (MDA) content; (B) hydrogen peroxide (H_2O_2); (C) superoxide dismutase (SOD) activity; and (D) catalase (CAT) activity in leaves from a cold-tolerant (G-69) and a cold-susceptible (G-51) accession of woodland strawberry after 0, 7, and 14 d of cold treatment. Control: temperature kept at 22 ± 3 °C with a 12 h photoperiod. The temperature in cold treatment was +2 °C during the dark period (12 h) and +7 °C during the light period (12 h) using the same light intensity and relative humidity as in the control treatment. Data represent the mean \pm SE of three biological replicates. Significant differences between G-69 and G-51 as per a Student *t*-test are indicated by **P*<0.05 and ***P*<0.01.

The cold-tolerant genotype G-69 deploys cold-adaptive genes more swiftly

We wondered how the superior cold resilience in G-69 would be reflected in the expression of stress-responsive genes. Therefore, we sampled representatives of cold signalling, the cold-induced transcription cascade, and COR genes as downstream targets (Fig. 4A). Cold signalling was represented by the jasmonate-response factor gene *JAZ9* (since cold stress activates jasmonate biosynthesis and since this member of the *JAZ* family had turned out to be induced during a preparatory study), and *MKKS*, a member of the second tier in the mitogen-activated protein kinase (MAPK) cascade modulating cold signalling, transcriptional activation, and cold responses. To probe for the activity of the transcription cascade, we measured the master switch *ICE1*, and its target factors *COLD BOX FACTOR 1 (CBF1)*, *DREB1E*, as well as *COLD BOX*

FACTOR 4 (CBF4) as a central regulator of cold acclimation. To monitor downstream responses, we scored *COR1* and *COR47*, along with the dehydrin *XERO2*, and *SUPEROXIDE DISMUTASE 1*. As housekeeping gene for normalization, we used *EF1 α* because the expression of this gene was constant over the entire set of time points, stress conditions, and genotypes (Supplementary Fig. S1). To visualize the abundance of different transcripts, we plotted relative transcript levels, based on the ΔC_t values (Fig. 4B). In addition, we plotted the fold values over the resting level, based on the $\Delta\Delta C_t$, to highlight inductive events (Fig. 4C).

The cold response of the two genotypes was clearly different. An early and transient induction of *JAZ9* transcripts was mainly seen in G-69, and much less in G-51. Under prolonged stress, *JAZ9* remained strongly elevated in G-69, but not in G-51. In contrast to *JAZ9*, *MKKS* transcripts remained

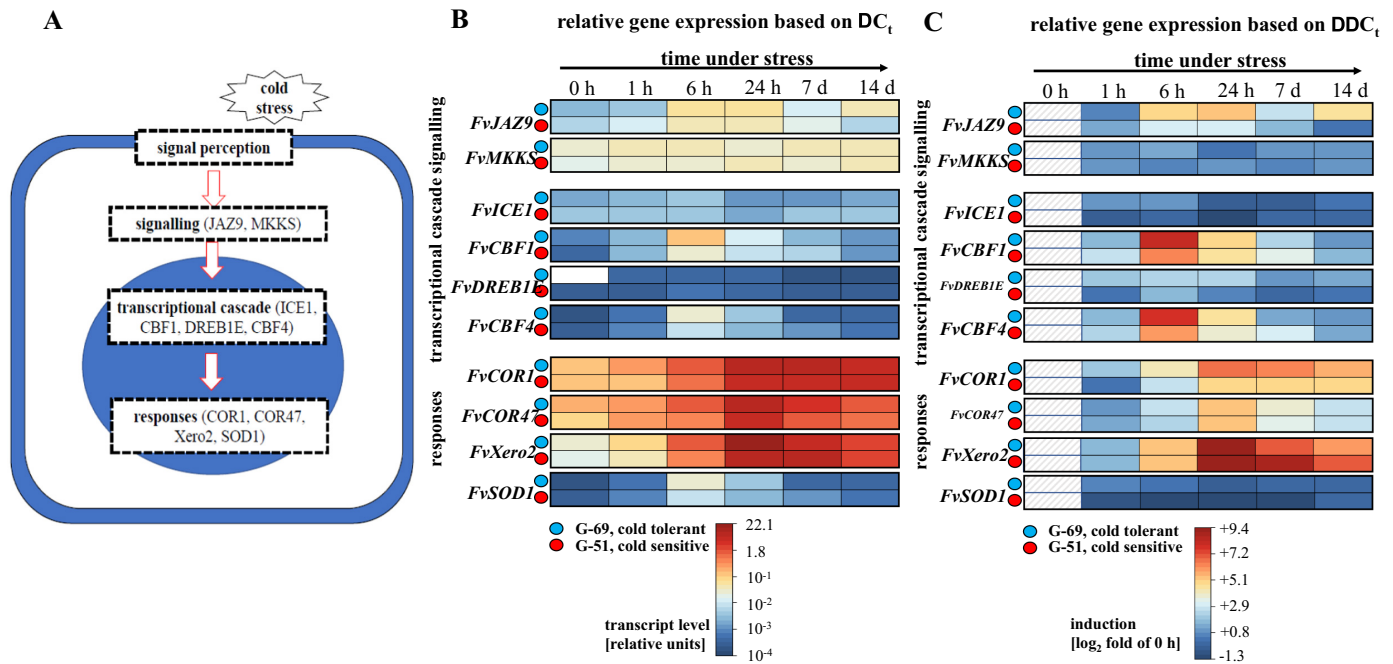


Fig. 4. Responses of cold stress-related transcripts in leaves from a cold-tolerant (G-69) and a cold-susceptible (G-51) accession of woodland strawberry. The temperature in cold treatment was +2 °C during the dark period (12 h) and +7 °C during the light period (12 h). (A) Rationale of the sampling. We used the jasmonate response factor JAZ9 and the kinase MAPKKS as readout for signalling, the master switch for cold-induced gene expression ICE1, along with its downstream targets Cold Box Factor 1, DREB1E, and the cold acclimation factor Cold Box Factor 4. To probe responses, we measured the cold response genes COR1 and COR47, the antifreezing dehydrin Xero2, and the ROS scavenger Superoxide Dismutase 1. (B) Time course of transcript accumulation under cold stress given in relative units (based on the ΔC_t values) to allow for comparison of transcript levels between genotypes and different genes. (C) Time course of transcript accumulation under cold stress given as induction factor over the initial level at 0 h (using $\Delta\Delta C_t$ values) to show the inducibility of a given transcript. Data represent means of three biological replicates, each in technical triplicates.

at more or less constant levels, irrespective of time and genotype. Specific and differential responses were also seen in the transcriptional cascade. Here, *ICE1* and *DREB1E* were not responsive, but *CBF1* showed a strong and transient induction, especially in G-69. The same pattern was observed for *CBF4*. Both transcripts peaked at 6 h after the onset of cold stress and thus coincided with the response of *JAZ9*. However, neither *CBF1* nor *CBF4* exhibited the late peak seen for *JAZ9* at late time points of cold stress. Among the downstream genes, a strong and persistent induction of the two *COR* genes as well as of the dehydrin gene *XERO2* was observed. For *COR1*, the induction was much stronger in G-69 as compared with G-51. For *COR47* and *XERO2*, the induction was comparable. However, ground levels in G-69 were already higher for both transcripts. Thus, the cold induction yielded more transcripts in G-69 for *COR47* and *XERO2*. The two *COR* genes and the dehydrin were induced later than their upstream regulators, *CBF1*, *CBF4*, and *JAZ9*. Transcripts for the important enzymatic antioxidant *SOD1* showed a mild and transient induction at 6 h, which was more prominent in G-69, but of minor amplitude if compared with the transcripts described above, matching the patterns observed for the activity of the SOD enzyme (Fig. 3C).

Cold stress changes the metabolic profiles of fruits and leaves differently

By untargeted GC×GC-MS analysis, we could separate and detect several hundred metabolites in strawberry fruits and leaves, covering primary metabolites such as sugars, sugar alcohols, sugar acids, amino acids, and organic acids, but also certain classes of secondary metabolites such as phenolic acids, catechins, sterols, and triterpenes. The GC×GC-MS chromatograms highlighted the high chemical diversity of the leaf metabolite profile (Supplementary Table S5). In fruit samples, fewer compounds were detected, and the chromatograms were dominated by high amounts of glucose, fructose, and sucrose (Supplementary Table S6).

For a general perspective on the complex patterns, we conducted a principal component analysis (Supplementary Fig. S2). The genotypes differed significantly even under control conditions, both for leaves and for fruits. Under stress, the response of the leaf metabolomes of the two genotypes converged, mainly because the cluster for G-69 under cold stress moved towards that of G-51 (which, albeit to a lesser extent, approximated the cluster for G-69). In the fruits, the metabolomes of the two genotypes shifted in parallel, such that the

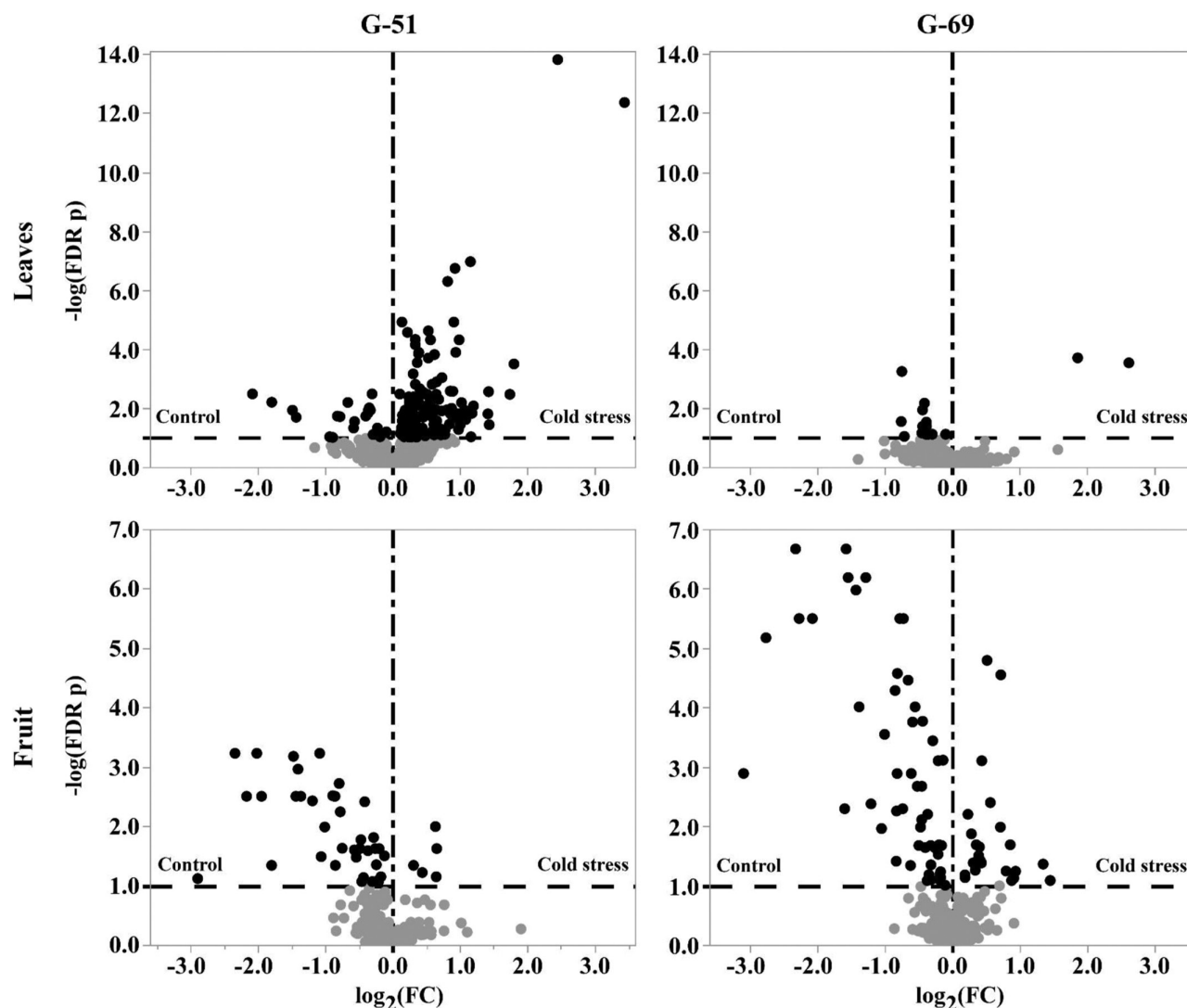


Fig. 5. Results of the ANOVA-based response screening analysis visualized by volcano plots. G-51, cold-sensitive genotype; G-69, cold-tolerant genotype. y-axis, significance given as the negatively log-transformed false discovery rate (FDR) P -value (i.e. FDR LogWorth). x-axis: \log_2 -transformed relative fold change (FC: cold stress/control). Each dot represents one analyte feature in a given plant organ and genotype. Positive and negative \log_2 FC values indicate higher concentrations in the cold stress or the control group, respectively.

distance between the genotypes remained comparable under both control and stress conditions.

To understand how the metabolic response to cold stress depends on genotype and organ, we used a visualization in the form of so-called volcano plots (Fig. 5). Here, leaves of G-51 were affected more significantly, with 138 leaf metabolites significantly elevated and 23 depleted after cold stress. In contrast, for G-69, only two metabolites were up-regulated, while 13 were down-regulated. In both genotypes, the accumulation of maltose (here quantified as two derivatives) was the response with the strongest amplitude. With regard to fruits, the volcano plots indicated a more comparable metabolic response of the two genotypes to cold stress. In the following sections, the

most relevant cold stress-triggered alterations in the metabolism of leaves and fruit will be described.

The full list of identified and quantified metabolites is given in [Supplementary Tables S5](#) and [S6](#). Many of them responded only slightly to the cold stress, and some showed similar responses regardless of the genotype. However, a substantial number were either quite different in their relative response or already quite different in their resting levels, allowing for correlation with cold susceptibility (G-51) or tolerance (G-69). In order to give a picture as complete as possible and to identify metabolic patterns, we plotted the data in the form of pathways giving both the relative abundance (normalized to the resting level of G-51) and the cold-induced change (as a percentage

of the resting level for the respective genotype). Below we describe these patterns, grouped by metabolite type.

Starch, cell wall, and citrate cycle are sustained more efficiently in leaves of G-69

While the most abundant sugars, sucrose, fructose, and glucose, appeared to be relatively buffered against cold stress (with resting levels that were 10–20% higher in G-69 over G-51), several salient features emerged (Fig. 6).

Cold stress induced maltose most strongly in G-51, indicating a greater need for starch mobilization. Likewise, xylose (indicating xylan breakdown from the cell wall) was significantly increased in G-51 but decreased in G-69. Resting levels of citrate cycle intermediates were higher in G-69. Cold stress induced fumarate and 2-oxoglutarate in G-51, while decreasing succinate, indicative of the γ -aminobutyric acid (GABA) shunt pathway. This GABA shunt seems less active in G-69. Raffinose, a well-known marker for osmotic stress (El Sayed *et al.*, 2014), and its precursor galactinol were induced in G-51, but not in G-69. Ascorbate was responsive as well. Here, G-51 increased dehydro-ascorbates to levels that were seen in G-69 already prior to cold stress. Compared with G-51, G-69 showed elevated ground levels for the compatible osmolytes glycerol and, prominently, glycosyl-glycerol. Although G-51 accumulated these compounds under cold stress, it was not able to reach the levels seen in G-69. A striking difference is the >7-fold higher ground levels of adenosine in G-69. Although these levels dropped under cold in G-69, while increasing in G-51, adenosine still remained ~3-fold higher in G-69 as compared with G-51.

Thus, G-69 seems more efficient in protecting carbohydrate polymers (starch, cell wall), in safeguarding the citrate cycle against stress-induced activation of the GABA shunt and maintaining a higher steady-state level of adenosine. It accumulates more glycerol and glycerol-glucoside than G-51, while G-51 relies on the stress markers galactinol and raffinose in response to cold stress.

Proline and GABA levels are strongly elevated in G-69 leaves already prior to stress

For amino acids and their derivatives (Fig. 7), two prominent changes emerged: under control conditions, proline levels in G-51 were very low and thus below the detection limit of the method but increased strongly under stress (the exact factor is not known, but if one assumes the noise threshold for the resting level, it would be >200-fold). The resting level in G-69 was comparable with the level reached by G-51 under stress. The second prominent difference was a >7-fold higher resting level of GABA in G-69 over that seen in G-51. Again, G-51 could make up under stress, but still reached only half of the value seen in G-69. While GABA might derive from the citrate cycle via the GABA shunt, this seems not to be the likely route, because the data from carbon metabolism show that this shunt pathway is less active in G-69 (Fig. 6). Instead, also glutamate,

which can feed both GABA and proline synthesis, shows elevated basal levels in G-69 as well as the concurrent derivative 2-oxoglutarate. Additional significant differences were found for the auxin precursor tryptophan, the glutathione precursor serine, its derivative ethanalamine, and the branched amino acids valine and isoleucine, an important cofactor in jasmonate signalling. For all of these amino acids, the ground levels in G-69 were considerably higher than in G-51 although G-51 could make up under stress, but only partially.

In summary, G-69 exhibits higher baseline levels of stress-responsive amino acids, while G-51 reached those levels (often only partially) after exposure to stress. This leads to the question of whether these *a priori* differences in amino acid metabolism are considered to be pre-adaptive, rendering G-69 more resilient to the challenges of cold stress.

The shikimate pathway is elevated in G-69 leaves prior to stress, and tyrosol is elevated after stress

The entry into the important phenylpropanoid pathway was strongly activated prior to stress in G-69 (Fig. 8). The precursor shikimate, its derivative phenylalanine, and its hydroxylated product tyrosine were much higher than in G-51, where these compounds accumulated to similar levels only under cold stress. Thus, the higher resting levels of these compounds in G-69 are of a pre-adaptive quality. In addition, these entrance molecules are also channelled to different routes. Tyrosol, a tyrosine derivative with strong antioxidant activity, was very low in G-69 prior to stress but doubled under cold stress, exceeding the levels in G-51. In contrast, vanillic acid generated from tyrosine by a concurrent pathway was strongly elevated in G-69 and persisted, while the lower levels in G-51 dropped even further. Thus, the striking pattern for tyrosol cannot be explained by differential partitioning of tyrosine to vanillic acid. Furthermore, the caffeic acid derivatives *m*-coumaric acid and ferulic acid (the first committed metabolite of monolignol biosynthesis) showed higher ground levels for G-69 but increased (and this only slightly) for G-51 under cold stress. In contrast, catechin and epicatechin were significantly lower in G-69, compared with G-51. It is noteworthy that there was an up-regulation of epicatechin in G-69 in response to cold stress, while in G-51 the level of this molecule is even somewhat decreased.

Overall, even in the absence of stress, G-69 sustains higher activity of the phenylpropanoid pathway, which appears to be directed to monolignols, but also to vanillic acid. In contrast, the branches leading to the catechins and tyrosol appear to be depleted in G-69, while the tyrosol branch is strongly activated and, to a minor extent, so too is the catechin pathway. Instead, the channelling of coumaric acid towards monolignols appears to be fairly buffered against cold stress. For G-51, the tyrosol and the catechin branches are more active prior to cold stress—tyrosol strongly (by 5-fold) and catechins mildly. These branches are suppressed under cold stress, and thus their response is a mirror image of the response seen in G-69.

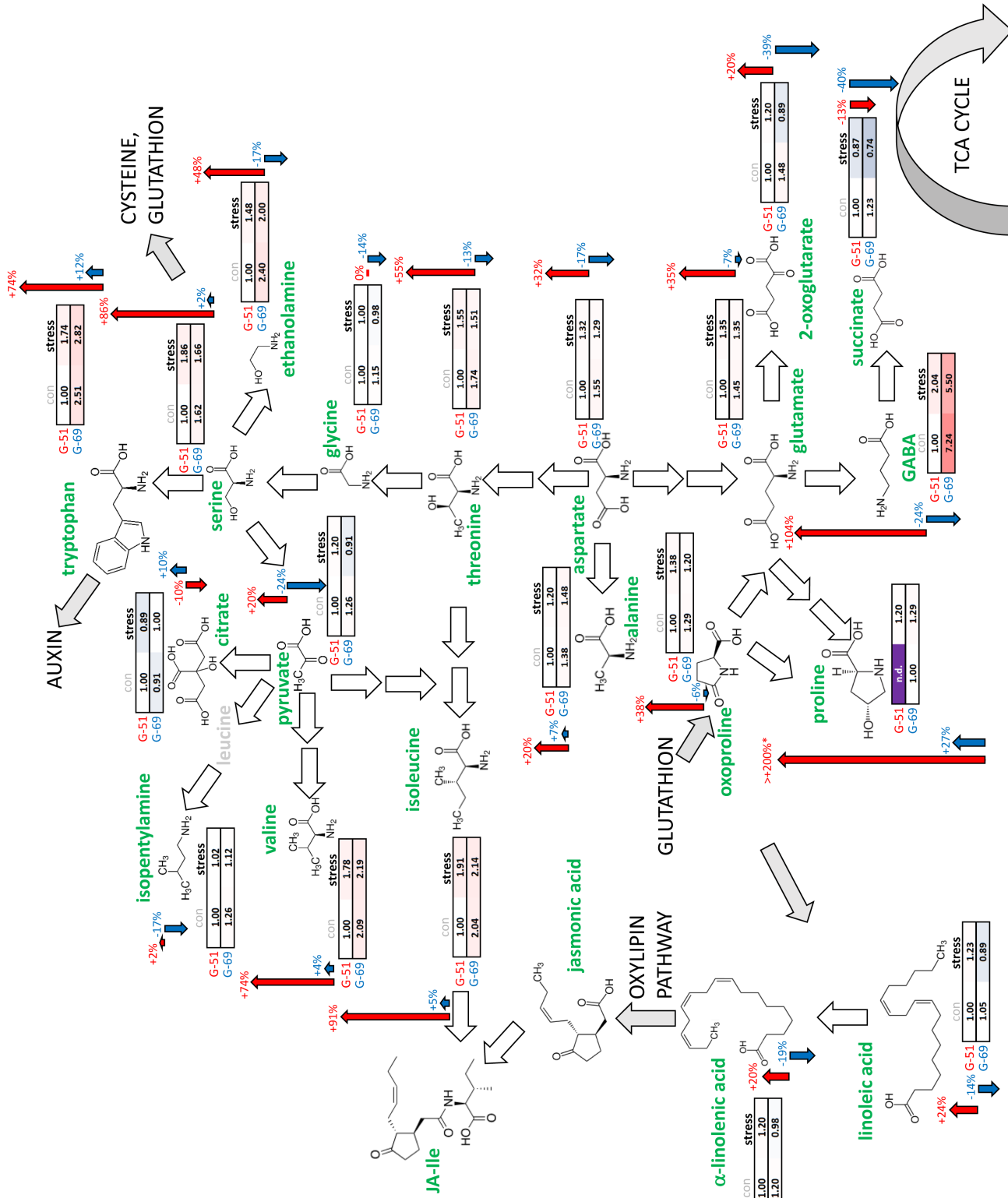


Fig. 7. Response of amino acid metabolism to cold stress in leaves from a cold-sensitive (G-51) and a cold-tolerant (G-69) accession of woodland strawberry. The temperature in cold treatment was +2 °C during the dark period (12 h) and +7 °C during the light period (12 h), as measured by GC-GC×MS. Metabolite abundance is given relative to the G-51 control. The change induced by the cold treatment relative to the respective control is indicated by the arrow (red G-51, blue G-69). Data represent 10 biological replicates. n.d. not detected, n.c.d. not consistently detected.

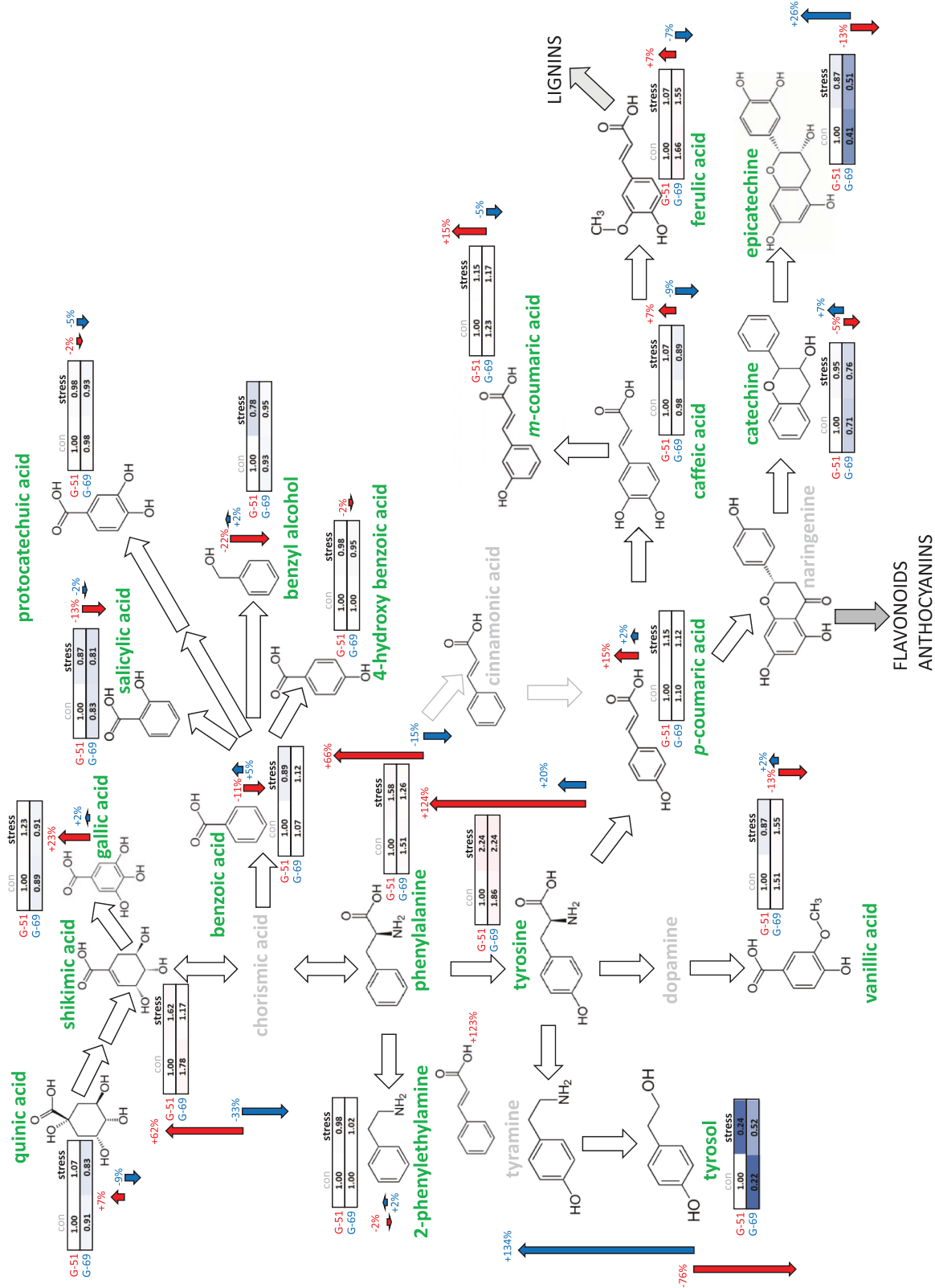


Fig. 8. Response of phenylpropanoids to cold stress in leaves from a cold-sensitive (G-51) and a cold-tolerant (G-69) accession of woodland strawberry. The temperature in cold treatment was +2 °C during the dark period (12 h) and +7 °C during the light period (12 h) as measured by GC-GC×MS. Metabolite abundance is given relative to the G-51 control. The change induced by the cold treatment relative to the respective control is indicated by the arrow (red G-51, blue G-69). Data represent 10 biological replicates. n.d. not detected, n.c.d. not consistently detected.

Specific terpenoids are elevated in G-69 leaves prior to cold stress

While our method was not tailored to detect terpenoids, we were able to detect significant changes among phytosterols that were already prevalent prior to cold stress (Fig. 9). In particular, (iso)fucosterol and neophytadiene isomers were conspicuously elevated in G-69 as compared with G-51. Under cold stress, these compounds increased in G-51, while decreasing in G-69, such that under cold stress comparable levels were reached in both genotypes. This pattern was specific, since β -sitosterol and α -tocopherol showed similar resting levels and only a minor cold response.

Effect of cold stress on the fruit metabolite profile is comparable in both genotypes

Unlike in the leaves (Supplementary Table S5), the two genotypes showed a comparable metabolic response of the fruits (Supplementary Table S6). It should be mentioned, however, that the fruits were exposed to cold stress after collection. Their responses therefore were not modulated by systemic signals from the leaves. Most amino acids were depleted under cold stress, while glutamine dropped by a factor of almost 10. Only tryptophan showed a significant increase in both genotypes (by about +50%), and to a more modest extent also cysteine and isoleucine. Among the organic acids, increased levels of pyruvate and β -hydroxybutyrate as well as slightly reduced levels of several citrate cycle metabolites (malate, succinate, fumarate, aconitate, and α -ketoglutarate, but not citrate) were notable. The main fruit sugars (glucose, fructose, and sucrose) remained unaffected by the cold treatment. A compound that might be ethyl glucoside, as well as some sugars eluting closely before the disaccharide region showed a strong increase in the genotype G-69, but only a weak, mostly insignificant response in G-51. In both genotypes, raffinose was only slightly up-regulated by cold stress. In contrast to the monomeric inositols, galactinol (i.e. 1- α -D-galactosyl-myo-inositol) was significantly lowered under stress in G-51. Several phenolic compounds as well as piperolic acid tended to become more abundant after cold stress in both genotypes but, again, significance was not always reached. Salicylate was mildly reduced in G-51.

Xero2 confers cold tolerance

Transcripts for dehydrin *Xero2* had been found to be *a priori* elevated in G-69 and also induced strongly and rapidly within 24 h after the onset of cold stress (Fig. 4). This pattern qualified the expression of *Xero2* as a marker associated with cold adaptation. To test this functionally, we cloned the coding sequence of *Xero2* from both genotypes (the coding sequences were identical) and generated fusions with GFP fused either N- or C-terminally, driven by the constitutive CaMV 35S promoter. These fusion constructs were transformed into tobacco BY-2 cells as host to address both the subcellular localization and a potential effect on cold tolerance of the host cells. For

both positions of the tag, the signal was seen in transvacuolar cytoplasmic strands and in the cortical cytoplasm subtending the plasma membrane, as well as in the perinuclear cytoplasm (Fig. 10A). It was also seen inside the nucleus but did not penetrate into the nucleolus. Since we collected confocal sections, contamination of this intranuclear signal by GFP from the perinuclear cytoplasm above or below the focal plane can be excluded. Since *Xero2* at \sim 20 kDa is a small protein, it remains, even in fusion with GFP, below the size exclusion limit for nuclear pores, which can explain why it can enter freely into the karyoplasm.

Since cold-induced mortality is an active process, whereby the challenged leaves are undergoing programmed cell death to ensure mobilization of resources to the meristem, we used a cold-stress relaxation experiment to address a potential role for *Xero2* in cold hardening. For this purpose, the cells were first challenged by ice water for 24 h to induce a robust level of cold stress. Subsequently, they were returned to 25 °C, such that the programmed cell death induced by this harsh stress could be executed (Fig. 10B). In fact, non-transformed tobacco BY-2 cells (WT) developed >40% mortality within 2 h after rewarming. The same was observed for controls, where GFP was fused to a non-related protein, tubulin α 3, expressed under the same promoter, CaMV 35S, using the same kanamycin resistance marker and the same selective conditions. For the *Xero2*-GFP overexpressors, the mortality was reduced by a factor of 4—these cells saturated at 12–13 mortality, irrespective of the position of the GFP tag. Thus, elevated levels of *Xero2* confer a robust tolerance against cold-inflicted cell death.

Discussion

In the current work we screened germplasm of a CWR of garden strawberry for cold tolerance and detected significant genetic variation. Using a pair of genotypes contrasting in cold tolerance, we identified CBF4, the dehydrin *Xero2*, and metabolic signatures as markers for cold tolerance. This work stimulates the following questions pursued below. What are genetic drivers of cold tolerance? What are the metabolic responses that mediate the effect of these drivers? What is different in the response of leaves and fruits? What can we do with this knowledge?

What are the drivers of cold tolerance?

Stress is defined as deviation from homeostasis that will lead to two possible outcomes (Selye, 1973): the system will, by feedback regulation, re-establish homeostasis or, if the challenge is too excessive, progressively lose homeostasis, culminating in the collapse of the entire system. Thus, the physiological and metabolic changes observed in response to stress can be of a 2-fold nature—either they might be manifestations of the

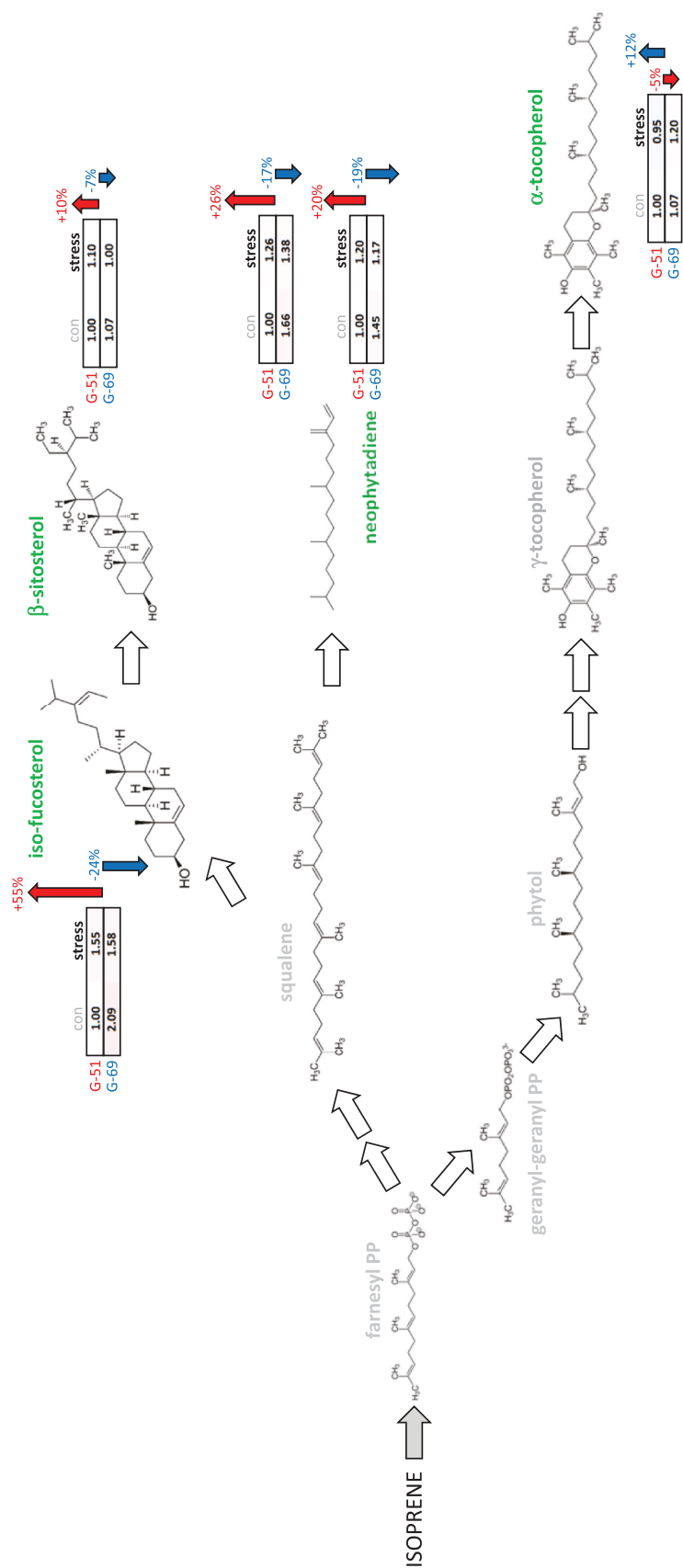


Fig. 9. Response of terpenoids to cold stress in leaves from a cold-sensitive (G-51) and a cold-tolerant (G-69) accession of woodland strawberry. The temperature in cold treatment was +2 °C during the dark period (12 h) and +7 °C during the light period (12 h) as measured by GC-GC×MS. Metabolite abundance is given relative to the G-51 control. The change induced by the cold treatment relative to the respective control is indicated by the arrow (red G-51, blue G-69). Data represent 10 biological replicates. n.d. not detected, n.c.d. not consistently detected.

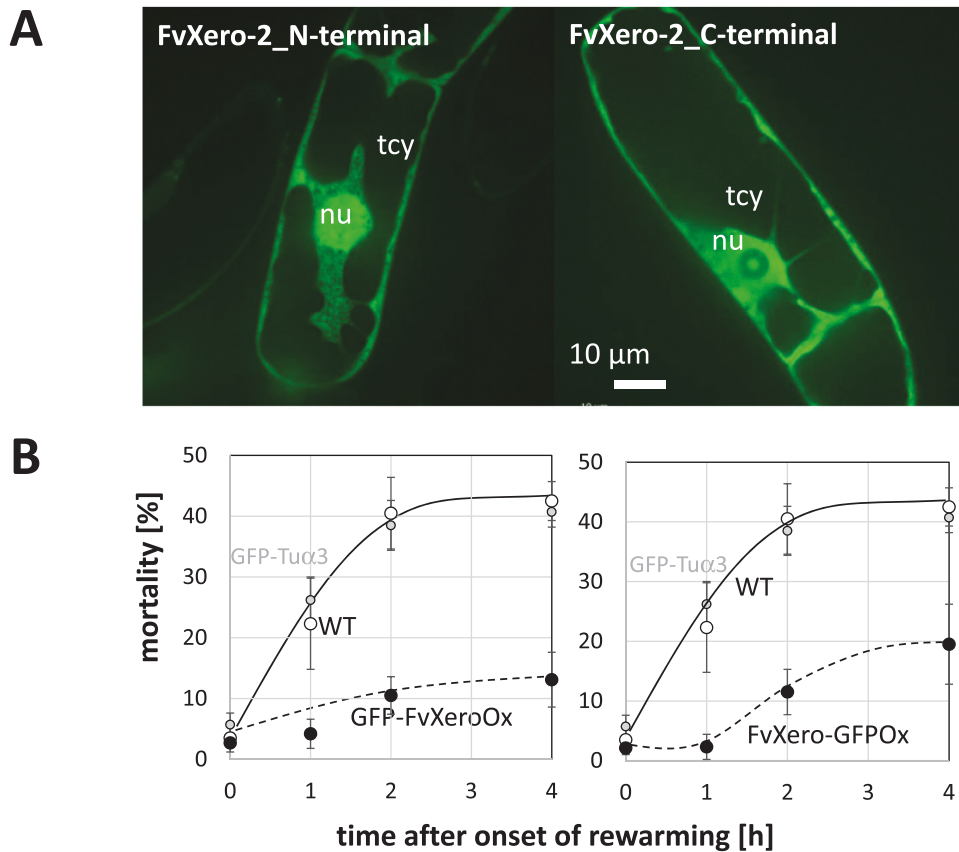


Fig. 10. Functional analysis of the dehydrin Xero2 from woodland strawberry upon heterologous expression in tobacco BY-2 cells as a host. (A) Subcellular localization of FvXero2 for fusion with GFP at the N-terminus (left) or the C-terminus (right). Representative images from confocal spinning disc microscopy are shown. (B) Cell mortality during recovery from a severe cold stress (20 h, 0 °C) in non-transformed tobacco BY-2 cells (WT), cells overexpressing GFP-tagged tobacco tubulin α 3 (GFP-Tu α 3), and cells overexpressing either the N-terminal (left) or the C-terminal (right) fusion of GFP to FvXero2. Data represent the mean and SE from three independent biological replicates.

processes activated to return to homeostasis (stress adaptation), or they might reflect the loss of homeostasis (stress damage). To assign a given stress-related event *per se* is not possible, but requires the functional context—does the stressed organism cope with the stress episode, or will it face irreversible damage? Comparing a pair of contrasting genotypes provides a logical filter to separate stress adaptation from stress damage. In the current study, we used the cold-tolerant genotype G-69 and the cold-susceptible genotype G-51 to identify adaptive events. These fall into two classes: class 1 comprises constitutive differences that are seen already prior to stress. The more robust enzymatic redox homeostasis in G-69 (Fig. 3) falls into this class, as do the elevated resting levels for components of MAPK signalling (*MKKS*), the cold transcription cascade (*DREB1E*), or the COR genes *COR47* and *Xero2* in G-69 (Fig. 4A). Both belong to the acidic subclass of dehydrins, proteins that are induced in many plants in response to cold stress and thought to act as cryoprotectants (Alsheikh *et al.*, 2005). Their lysine-rich repeat sequence forms an amphipathic α -helix allowing interaction with lipids, enabling protection of membranes from freezing damage (Close, 1996). The dehydrin *COR47* was

already found to be up-regulated in acclimated plants during a study comparing different strawberry species with respect to freezing tolerance (Davik *et al.*, 2013), and contains a serine-rich motif that can bind calcium upon cold-induced phosphorylation (Alsheikh *et al.*, 2005). In contrast, Xero2 (also known as LTI30) belongs to the glycine-rich class of dehydrins lacking those serines and is, therefore, not regulated by phosphorylation. Its lysine-rich repeats interact electrostatically with the negatively charged phosphate groups of membrane lipids, sustaining membrane stability under drought and under freezing (Gupta *et al.*, 2019; Andersson *et al.*, 2020), which is the most straightforward explanation for our finding that ectopic expression of *FvXero2* can render tobacco BY-2 cells cold tolerant (Fig. 10) as compared with non-transformed wild type, but also compared with a line overexpressing a GFP fusion of a non-related protein, tubulin α 3, under the same selective conditions.

Class 2 comprises events that do not differ under control conditions, but are more vigorously induced under stress (Fig. 4B). Salient examples are CBF1, a member of the cold signalling cascade, and CBF4, known as a regulator of cold hardening

in several plants, including strawberry (Koehler *et al.*, 2012) and grapevine (Tillett *et al.*, 2012; Shi *et al.*, 2022). Both are activated by the master switch ICE1 (reviewed in Chinnusamy *et al.*, 2007) and address partially different sets of COR genes (Shi *et al.*, 2017). In this context, CBF4 is of special interest, because, here, the functional context with cold acclimation has been established for a couple of plants (Haake *et al.*, 2002; Koehler *et al.*, 2012; Tillett *et al.*, 2012; Shi *et al.*, 2022).

Thus, a pre-adaptive accumulation of a COR gene and a more efficient induction of a positive regulator appear to be the central drivers for the superior cold tolerance in G-69.

What is the leaf metabolic signature of cold resilience?

Induction of the dehydrin Xero2 can be understood as a protective measure, safeguarding membranes from freezing damage. However, even non-freezing temperatures will perturb metabolic homeostasis, culminating in progressive damage. The responses of *CBF1* and *CBF4* herald subsequent metabolic changes. Leaves of the tolerant genotype accumulated less MDA as readout for oxidative damage, associated with a swifter and stronger activation of SOD and catalase, and showed a contrasting metabolic response. Our comparative design allows us to interpret these metabolic responses as either manifestations of stress damage or stress adaptation. In the following, we will discuss the salient differences, integrate them into the literature record, and come up with mechanistic explanations for their role in cold susceptibility versus tolerance.

The more robust redox homeostasis in G-69 is mirrored by elevated resting levels for intermediates of the citrate cycle including malate, citramalate, succinate, fumarate, and 2-oxoglutarate (Fig. 6). The substantial increase of succinate and 2-oxoglutarate under stress shows that G-69, in sharp contrast to G-51, can buffer the oxidative challenge and does not rely on the GABA shunt as a salvage strategy. The GABA shunt is turned on when mitochondria face oxidative stress (especially the accumulation of superoxide), promoting retrograde signalling and activating the alternative oxidase pathway, which will turn on the GABA shunt (reviewed in Bandehagh and Taylor, 2020).

The strong and rapid induction of β -amylase, breaking down starch into maltose, during cold stress is a well-known phenomenon and has been proposed to provide the cell with a compatible osmolyte to resist the formation of ice crystals, but also to buffer photosynthesis (Kaplan and Guy, 2004). This phenomenon directly illustrates to what extent the plant needs to rely on resource mobilization to sustain homeostasis. Maltose is thus a direct proxy for the degree of cold stress. The fact that G-51 has to rely on starch breakdown to a higher extent than G-69 is consistent with this interpretation.

The strong accumulation of adenosine in G-69 indicates a strong activity of the purine salvage pathway as compared with catabolic breakdown to mobilize ammonium (reviewed in Zrenner *et al.*, 2006). This allows recruitment of adenosine

for other purposes, such as the synthesis of cytokinins, activating the adaptation to cold stress (Jeon *et al.*, 2010).

We also interpret the higher accumulation of glycerol and glycerol-glucoside in G-69 as an adaptive response. The formation of this compatible solute in response to stress seems to be an evolutionarily ancient acquisition, since it is already found in cyanobacteria (Ferjani *et al.*, 2003). Overexpression of the respective synthase confers stress tolerance (Klähn *et al.*, 2009). Due to a more efficient buffering of the citrate cycle, G-69 can 'afford' to feed glycerol-glucoside synthesis, while G-51, feeding the GABA shunt, needs to rely on the more expensive stress markers galactinol and raffinose instead (Nishizawa *et al.*, 2008).

Cold tolerance in G-69 correlates with high resting levels of proline, reached in G-51 only in response to cold stress. Accumulation of proline is a well-known stress response and provides osmoprotection as well as ROS scavenging (for a classical review, see Verbruggen and Hermans, 2008). Recently, differences in proline resting levels were shown to determine basal freezing tolerance (Hoermiller *et al.*, 2022), congruent with our data. The same pattern is seen for GABA—this non-proteinogenic amino acid accumulates in response to various stresses (for a review, see Shelp *et al.*, 2017) and coordinates antioxidative defence. Exogenous GABA can render chilling-sensitive tomato cold tolerant (Abd Elbar *et al.*, 2021), and correlates with cold hardness in wheat and barley (Mazzucotelli *et al.*, 2006). The 7-fold higher ground levels of GABA in G-69 are, therefore, a clear readout for cold tolerance.

Both the shikimate pathway, leading to, and the phenylpropanoid pathway, deriving from phenylalanine is more active in G-69 *a priori*. Tyrosol, a strong antioxidant (Yen and Hsieh, 1997), deviates from the general pattern. Overexpression of tyrosine decarboxylase, the enzyme generating tyrosol, confers stress tolerance in apples, a member of the same family as strawberry (Liu *et al.*, 2021). In the cold-sensitive olive, tyrosol levels increase under mild cold stress, but then drop sharply to increase stress stringency (Ortega-García and Peragón, 2009). Thus, the high resting levels of tyrosol in G-51 are indicators that this genotype was already under mild cold stress prior to the experiment; the suppression during the experiment is a hallmark of severe stress. In contrast, G-69 was responding to the same treatment as a mild stress, and thus induced the accumulation of tyrosol.

The significantly increased resting levels of the antioxidant neophytadiene (Bhardwaj *et al.*, 2020) in G-69 can be interpreted as an anticipative response, because G-51 induces neophytadiene only in response to stress. Likewise, the 2-fold higher resting levels of fucosterol seem to be a hallmark of cold tolerance. This sterol species has been proposed to sustain membrane fluidity under cold stress (Mouritsen *et al.*, 2017).

Overall, breakdown of starch and the cell wall are hallmarks of cold sensitivity and seem to be a salvage pathway to generate compatible osmolytes. Instead, a more robust buffering of the citrate cycle, strong induction of adenosine, a constitutive accumulation

of proline (compatible osmolyte and antioxidant) and GABA (coordinating signal for cold acclimation), a higher activity of the shikimate pathway and phenylpropanoid biosynthesis, as well as a more pronounced accumulation of fucosterol (membrane fluidity) and of neophytadiene (antioxidant) can be considered as anticipative responses preparing G-69 for cold stress. Instead, the higher resting levels of tyrosol (antioxidant) in G-51 along with the inverted cold response in the two genotypes indicate that the oxidative level in G-51 is elevated even under resting levels.

How do metabolic signatures of fruits differ from those seen in the leaves?

The metabolic patterns in the fruits (Supplementary Table S6) differ fundamentally from those seen in the leaves, possibly because they draw their energy from respiration rather than from photosynthesis. Their metabolic patterns are relevant for post-harvest physiology. The strong decline of amino acids, opposite to the situation in leaves, indicates channelling of free amino acids into other pathways.

While other amino acids decline, tryptophan clearly accumulates. Tryptophan is the direct precursor for the central dicot pathway yielding the auxin indole-3-acetic acid (Zhao, 2012). The activation of fruit growth by indole-3-acetic acid generated by the achenes has been a classic model for auxin effects (Dollfus, 1936; Nitsch, 1950). Auxin remains relevant in mature fruits and accumulates under cold stress, while, simultaneously, abscisic acid is depleted. The functional context of this auxin accumulation cannot be fruit growth since the fruits are already fully expanded. However, auxins act as negative regulators for cell wall breakdown by repression of both endo-1,4- β -glucanase (Harpster *et al.*, 1998) and polygalacturonase (Villareal *et al.*, 2009), and thus delay the softening of mature fruits.

From the perspective of fruit quality, several aspects are noteworthy. The ratio of sugars over acids as an important sensory parameter did not change much, because both sugars and acids remained mostly constant. However, amino acids, as crucial precursors of numerous flavour compounds (for a review, see Siegmund, 2015), are generally down-modulated under cold stress, which should impair strawberry aroma, similar to tomato under refrigeration (Farneti *et al.*, 2015; Zhang *et al.*, 2016). For strawberry, the effect of chemical compounds related to cold adaptation, such as glycine betaine, trehalose, salicylic acid, and proline, has been assessed, with the most significant effect observed for salicylic acid (Roussos *et al.*, 2020). However, these studies were conducted in a single genotype, such that it is difficult to separate chilling damage from adaptation.

What can we do with this knowledge?

Using woodland strawberries as CWRs, we have identified genotypes that are endowed with a good level of freezing tolerance, and we could relate this freezing tolerance to a swifter activation of specific transcriptional regulators (CBF1 and CBF4),

but also with an anticipative activation of the dehydrin Xero2. These changes are not linked with alterations of the coding sequence, but with altered patterns of expression, a common pattern for resilience factors recovered in CWRs. For instance, a specific genotype of the European wild grapevine, the ancestor of domesticated grapevine, was found to exhibit partial resistance against downy mildew linked with a superior inducibility of stilbene synthases that could be assigned to an ancestral allele of a promoter driving the transcriptional activator MYB14, a key regulator for stilbene synthases (Duan *et al.*, 2015, 2016). Once identified, such 'wild' promoter alleles could be introgressed into a domesticated crop using marker-assisted selection based on the sequence information indicative of the wild allele (here, the alleles for Xero2, CBF1, and CBF4 from G-69). This strategy has been successful in generating rice varieties that combine high yield and local taste preferences with resilience to salinity, flooding, or invading pests, introgressing respective quantitative trait loci from traditional landraces or even from CWRs (for a review, see Collar and Mackill, 2008). To apply this strategy to the octaploid garden strawberry is challenging, though. However, recent advances in genomics and the vigorous impact of genetic markers on breeding of garden strawberry have enabled remarkable breakthroughs that have shortened the breeding cycle to 2–3 years (for a review, see Whitaker *et al.*, 2020).

Supplementary data

The following supplementary data are available at [JXB online](#).

Table S1. Scoring of freezing damage.

Table S2. Oligonucleotide primers used for qPCR analysis.

Table S3. Temperature and rainfall in Karlsruhe during 2020.

Table S4. Parameters of the untargeted GC \times GC-MS metabolome analysis.

Table S5. Metabolites in fruits of G-69 and G-51.

Table S6. Metabolites in fruits of G-69 and G-51.

Fig. S1. Expression of *FvEF1 α* in leaves from G-69 and G-51.

Fig. S2. Principal component analysis of leaf and fruit metabolome.

Acknowledgements

Professional help with plant cultivation from Joachim Daumann, Annaliese Kuppinger, and Siegfried Bendel from the Experimental Station of the Joseph Kölreuter Institute for Plant Sciences at the Karlsruhe Institute of Technology is gratefully acknowledged, as is excellent technical assistance with GC metabolomics by Silvia Remmert, Michael Meyer, and Lea Böckstiegel at the metabolomics lab of the Max Rubner Institute.

Author contributions

AK and PN: conceptualization, germplasm screening and selection; AK, CW, and PN: methodology, data curation, data analysis, and manuscript

preparation; AK: data validation; AK, CW, TL, DK, and EA: experimental work; PN, MH, and FK: funding acquisition; SK and PN: infrastructure; AK, PN, CW, SK, and MH: editing.

Conflict of interest

The authors declare that there are no conflicts of interest.

Funding

This work was supported by funds from the German Federal Ministries of Education and Research and Agriculture, Nutrition and Consumer Protection (BMBF; project Fragananas, BMELV, WEL Genbank), and the Egyptian STDF (project 22984).

Data availability

All data are given in the manuscript and the supplementary data.

References

- Abbo S, Pinhasi van-Oss R, Gopher A, Saranga Y, Ofner I, Peleg Z.** 2014. Plant domestication versus crop evolution: a conceptual framework for cereals and grain legumes. *Trends in Plant Science* **19**, 351–360.
- Abd Elbar OH, Elkelish A, Niedbala G, et al.** 2021. Protective effect of γ -aminobutyric acid against chilling stress during reproductive stage in tomato plants through modulation of sugar metabolism, chloroplast integrity, and antioxidative defense systems. *Frontiers in Plant Science* **12**, 663750.
- Aebi H.** 1984. Catalase in vitro. *Methods in Enzymology* **105**, 121–126.
- Aghdam MS, Sayyari M, Luo ZS.** 2021. Exogenous phyto-sulfokine α application delays senescence and promotes antioxidant nutrient accumulation in strawberry fruit during cold storage by triggering endogenous phyto-sulfokine α signaling. *Postharvest Biology and Technology* **175**, 111473.
- Alsheikh MK, Svensson JT, Randall SK.** 2005. Phosphorylation regulated ion-binding is a property shared by the acidic subclass dehydrins. *Plant, Cell & Environment* **28**, 1114–1122.
- Andersson JM, Pham QD, Mateos H, Eriksson S, Harryson P, Sparr E.** 2020. The plant dehydrin Lti30 stabilizes lipid lamellar structures in varying hydration conditions. *Journal of Lipid Research* **61**, 1014–1024.
- Arafat N.** 2019. Battle of the strawberries. www.madamas.com/en/2019/12/25/feature/society/battle-of-the-strawberries/ Accessed 20 April 2023.
- Asghari M, Hasanlooe AR.** 2015. Interaction effects of salicylic acid and methyl jasmonate on total antioxidant content, catalase and peroxidase enzymes activity in ‘Sabrosa’ strawberry fruit during storage. *Scientia Horticulturae* **197**, 490–495.
- Augsburger CK.** 2013. Reconstructing patterns of temperature, phenology, and frost damage over 124 years: spring damage risk is increasing. *Ecology* **94**, 41–50.
- Ayala-Zavala JF, Wang SY, Wang CY, Gonzalez-Aguilar GA.** 2005. Methyl jasmonate in conjunction with ethanol treatment increases antioxidant capacity, volatile compounds and postharvest life of strawberry fruit. *European Food Research and Technology* **221**, 731–738.
- Bandehagh A, Taylor NL.** 2020. Can alternative metabolic pathways and shunts overcome salinity induced inhibition of central carbon metabolism in crops? *Frontiers in Plant Science* **11**, 1072.
- Beauchamp C, Fridovich I.** 1971. Superoxide dismutase: improved assays and an assay applicable to acrylamide gels. *Analytical Biochemistry* **44**, 276–287.
- Bhardwaj M, Sali VK, Sugumar M, Vasanthi HR.** 2020. Neophytadiene from *Turbinaria ornata* suppresses LPS-induced inflammatory response in RAW 264.7 macrophages and Sprague–Dawley rats. *Inflammation* **43**, 937–950.
- Borgmann P, Oevermann S, Friesen N, Zachgo S.** 2014. oppeDie Genbank für Wildpflanzen für Ernährung und Landwirtschaft (WEL). *Hoppea special issue*, 41–69.
- Bradford MM.** 1976. A rapid and sensitive method for the quantitation of microgram quantities of protein utilizing the principle of protein–dye binding. *Analytical Biochemistry* **72**, 248–254.
- Brizzolara S, Hertog M, Tosetti R, Nicolai B, Tonutti P.** 2018. Metabolic responses to low temperature of three peach fruit cultivars differently sensitive to cold storage. *Frontiers in Plant Science* **9**, 706.
- Chinnusamy V, Zhu J, Zhu JK.** 2007. Cold stress regulation of gene expression in plants. *Trends in Plant Science* **12**, 444–451.
- Close TJ.** 1996. Dehydrins: emergence of a biochemical role of a family of plant dehydration proteins. *Physiologia Plantarum* **97**, 795–803.
- Collard BC, Mackill DJ.** 2008. Marker-assisted selection: an approach for precision plant breeding in the twenty-first century. *Philosophical Transactions of the Royal Society B: Biological Sciences* **363**, 557–572.
- Cortés AJ, López-Hernández F.** 2021. Harnessing crop wild diversity for climate change adaptation. *Genes* **12**, 783.
- Datir S, Yousef S, Sharma S, Kochle M, Ravikumar A, Chugh J.** 2020. Cold storage reveals distinct metabolic perturbations in processing and non-processing cultivars of potato (*Solanum tuberosum* L.). *Nature Scientific Reports* **10**, 6268.
- Davik J, Koehler G, From B, Torp T, Rohloff J, Eidem P, Wilson RC, Sonstebj A, Randall SK, Alsheikh M.** 2013. Dehydrin, alcohol dehydrogenase, and central metabolite levels are associated with cold tolerance in diploid strawberry (*Fragaria* spp.). *Planta* **237**, 265–277.
- Delgado-Vargas F, Vega-Álvarez M, Landeros Sánchez A, López-Angulo G, Salazar-Salas NY, Quintero-Soto MF, Pineda-Hidalgo KV, López-Valenzuela JA.** 2022. Metabolic changes associated with chilling injury tolerance in tomato fruit with hot water pretreatment. *Journal of Food Biochemistry* **46**, e14056.
- Dollfus H.** 1936. Wuchsstoffstudien. *Planta* **25**, 1–21.
- do Nascimento Nunes MC, Morais AMMB, Brecht J, Sargent S.** 1995. Quality of strawberries after storage is reduced by a short delay to cooling. In: *Proceedings of the International Conference of Harvest and Postharvest Technologies for Fresh Fruits and Vegetables Guanajuato, Mexico*, 15–22.
- Duan D, Fischer S, Merz PR, Bogs J, Riemann M, Nick P.** 2016. An ancestral allele of grapevine transcription factor MYB14 promotes plant defence. *Journal of Experimental Botany* **67**, 1795–1804.
- Duan D, Halter D, Baltenweck R, Tisch C, Tröster V, Kortekamp A, Hugueney P, Nick P.** 2015. Genetic diversity of stilbene metabolism in *Vitis sylvestris*. *Journal of Experimental Botany* **66**, 3243–3257.
- El Sayed AI, Rafudeen MS, Gollack D.** 2014. Physiological aspects of raffinose family oligosaccharides in plants: protection against abiotic stress. *Plant Biology* **16**, 1–8.
- Farneti B, Alarcón AA, Papatotiriou FG, Samudrala D, Cristescu SM, Costa G, Harren FJM, Woltering EJ.** 2015. Chilling-induced changes in aroma volatile profiles in tomato. *Food and Bioprocess Technology* **8**, 1442–1454.
- Ferjani A, Mustardy L, Sulpice R, Marin K, Suzuki I, Hagemann M, Murata N.** 2003. Glucosylglycerol, a compatible solute, sustains cell division under salt stress. *Plant Physiology* **131**, 1628–1637.
- Fuller MP, Telli G.** 2008. An investigation of the frost hardiness of grapevine (*Vitis vinifera*) during bud break. *Annals of Applied Biology* **135**, 589–595.
- Gaff D, Okong’O-Ogola O.** 1971. The use of non-permeating pigments for testing the survival of cells. *Journal of Experimental Botany* **22**, 756–758.
- Gao N, Wadhvani P, Mühlhäuser P, Liu Q, Riemann M, Ulrich AS, Nick P.** 2016. An antifungal protein from *Ginkgo biloba* binds actin and can trigger cell death. *Protoplasma* **253**, 1159–1174.
- Gupta A, Marzinek JK, Jefferies D, Bond PJ, Harryson P, Wohland T.** 2019. The disordered plant dehydrin Lti30 protects the membrane during

- water-related stress by cross-linking lipids. *Journal of Biological Chemistry* **294**, 6468–6482.
- Guy CL.** 1990. Cold acclimation and freezing stress tolerance: role of protein metabolism. *Annual Review of Plant Physiology and Plant Molecular Biology* **41**, 187–223.
- Haake V, Cook D, Riechmann JL, Pineda O, Thomashow MF, Zhang JZ.** 2002. Transcription factor CBF4 is a regulator of drought adaptation in *Arabidopsis*. *Plant Physiology* **130**, 639–648.
- Hajjar R, Hodgkin T.** 2007. The use of wild relatives in crop improvement: a survey of developments over the last 20 years. *Euphytica* **156**, 1–13.
- Harpster MH, Brummell DA, Dunsmuir P.** 1998. Expression analysis of a ripening-specific, auxin-repressed endo-1,4- β -glucanase gene in strawberry. *Plant Physiology* **118**, 1307–1316.
- Hatoum D, Annaratone C, Hertog MLATM, Geeraerd AH, Nicolai BM.** 2014. Targeted metabolomics study of 'Braeburn' apples during long-term storage. *Postharvest Biology and Technology* **96**, 33–41.
- Heath RL, Packer L.** 1968. Photoperoxidation in isolated chloroplasts. *Archives in Biochemistry and Biophysics* **125**, 850–857.
- Hoermiller II, Funck D, Schönewolf L, May H, Heyer AG.** 2022. Cytosolic proline is required for basal freezing tolerance in *Arabidopsis*. *Plant, Cell & Environment* **45**, 147–155.
- Irkaeva NM, Ankudinova IN.** 1994. Evaluation of the outbreeding level of the strawberry *Fragaria vesca* L. using genetic markers. *Genetika* **30**, 816–822.
- Jeon J, Kim NY, Kim S, et al.** 2010. A subset of cytokinin two-component signaling system plays a role in cold temperature stress response in *Arabidopsis*. *Journal of Biological Chemistry* **285**, 23371–23386.
- Kaplan F, Guy CL.** 2004. β -Amylase induction and the protective role of maltose during temperature shock. *Plant Physiology* **135**, 1674–1684.
- Klähn S, Marquardt DM, Rollwitz I, Hagemann M.** 2009. Expression of the *gppPS* gene for glucosylglycerol biosynthesis from *Azotobacter vinelandii* improves the salt tolerance of *Arabidopsis thaliana*. *Journal of Experimental Botany* **60**, 1679–1689.
- Kodra E, Steinhäuser K, Ganguly AR.** 2011. Persisting cold extremes under 21st-century warming scenarios. *Geophysical Research Letters* **38**, L08705.
- Koehler G, Wilson RC, Goodpaster JV, Sønsteby A, Lai XY, Witzmann FA, You JS, Rohloff J, Randall SK, Alsheikh M.** 2012. Proteomic study of low-temperature responses in strawberry cultivars (*Fragaria* \times *ananassa*) that differ in cold tolerance. *Plant Physiology* **159**, 1787–1805.
- Kumagai F, Yoneda A, Tomida T, Sano T, Nagata T, Hasezawa S.** 2001. Fate of nascent microtubules organized at the M/G1 interphase, as visualized by synchronized tobacco BY-2 cells stably expressing GFP-tubulin: time-sequence observations of the reorganization of cortical microtubules in living plant cells. *Plant and Cell Physiology* **42**, 723–732.
- Liu X, Jin Y, Tan K, Zheng J, Gao T, Zhang Z, Zhao Y, Ma F, Li C.** 2021. *MdTyDc* overexpression improves alkalinity tolerance in *Malus domestica*. *Frontiers in Plant Science* **12**, 625890.
- Livak KJ, Schmittgen TD.** 2001. Analysis of relative gene expression data using real-time quantitative PCR and the $2^{-\Delta\Delta C_T}$ method. *Methods* **25**, 402–408.
- Lv J, Zheng T, Song Z, Pervaiz T, Dong T, Zhang Y, Jia H, Fang J.** 2022. Strawberry proteome responses to controlled hot and cold stress partly mimic post-harvest storage temperature effects on fruit quality. *Frontiers in Nutrition* **8**, 812666.
- Lyons JM.** 1973. Chilling injury in plants. *Annual Review of Plant Physiology* **24**, 445–466.
- Ma Y, Dai X, Xu Y, et al.** 2015. COLD1 confers chilling tolerance in rice. *Cell* **160**, 1209–1221.
- Mazzucotelli E, Tartari A, Cattivelli L, Forlani G.** 2006. Metabolism of gamma-aminobutyric acid during cold acclimation and freezing and its relationship to frost tolerance in barley and wheat. *Journal of Experimental Botany* **57**, 3755–3766.
- Molisch H.** 1897. *Untersuchungen über das Erfrieren der Pflanzen*. Jena: Gustav Fischer Verlag.
- Mouritsen OG, Bagatolli LA, Duelund L, Garvik O, Ipsen JH, Simonsen AC.** 2017. Effects of seaweed sterols fucosterol and desmosterol on lipid membranes. *Chemistry and Physics of Lipids* **205**, 1–10.
- Neuwald DA, Grötzinger M, Wood R, Kitemann D, Wünsche J.** 2021. Comparison of two strawberry postharvest handling strategies: rapidly cooled or non-cooled fruit to the distributor. *Acta Horticulturae* **1309**, 835–840.
- Nishizawa A, Yabuta Y, Shigeoka S.** 2008. Galactinol and raffinose constitute a novel function to protect plants from oxidative damage. *Plant Physiology* **147**, 1251–1263.
- Nitsch JP.** 1950. Growth and morphogenesis of the strawberry as related to auxin. *American Journal of Botany* **37**, 211–215.
- Ortega-García F, Peragón J.** 2009. Phenylalanine ammonia-lyase, polyphenol oxidase, and phenol concentration in fruits of *Olea europaea* L. cv. Picual, Verdial, Arbequina, and Frantoio during ripening. *Journal of Agricultural and Food Chemistry* **57**, 10331–10340.
- Romo-Pérez ML, Weinert CH, Häußler M, Egert B, Frechen MA, Trierweiler B, Kulling SE, Zörb C.** 2020. Metabolite profiling of onion landraces and the cold storage effect. *Plant Physiology and Biochemistry* **146**, 428–437.
- Roussos PA, Ntanos E, Tsafouros A, Denaxa NK.** 2020. Strawberry physiological and biochemical responses to chilling and freezing stress and application of alleviating factors as countermeasures. *Journal of Berry Research* **10**, 437–457.
- Schneider N, Ludwig H, Nick P.** 2015. Suppression of tubulin deetyrosination by parthenolide recruits the plant specific kinesin KCH to cortical microtubules. *Journal of Experimental Botany* **66**, 2001–2011.
- Selye H.** 1973. The evolution of the stress concept. *American Scientist* **61**, 692–699.
- Shelp BJ, Bown AW, Zarei A.** 2017. 4-Aminobutyrate (GABA): a metabolite and signal with practical significance. *Botany* **95**, 1015–1032.
- Shi SY, Wang G, Wang YD, Zhang LG, Zhang LX.** 2005. Protective effect of nitric oxide against oxidative stress under ultraviolet-B radiation. *Nitric Oxide* **13**, 1–9.
- Shi W, Riemann M, Rieger SM, Nick P.** 2022. Is cold-induced nuclear import of CBF4 regulating freezing tolerance? *International Journal of Molecular Science* **23**, 1141.
- Shi Y, Ding Y, Yang S.** 2018. Molecular regulation of CBF signaling in cold acclimation. *Trends in Plant Science* **23**, 623–637.
- Shi Y, Huang J, Sun T, Wang X, Zhu C, Ai Y, Gu H.** 2017. The precise regulation of different COR genes by individual CBF transcription factors in *Arabidopsis thaliana*. *Journal of Integrative Plant Biology* **59**, 118–133.
- Siegmund B.** 2015. Biogenesis of aroma compounds: flavour formation in fruits and vegetables. In: Parker JK, Elmore JS, Methven J, eds. *Flavour development, analysis and perception in food and beverages*. Sawston, UK: Woodhead Publishing, 127–149.
- Svyatyna K, Jikumaru Y, Brendel R, Reichelt M, Mithoefer A, Takano M, Kamiya Y, Nick P, Riemann M.** 2014. Light induces jasmonate–isoleucine conjugation via OsJAR1-dependent and-independent pathways in rice. *Plant, Cell & Environment* **37**, 827–839.
- Tillett RL, Wheatley MD, Tattersall EA, Schlauch KA, Cramer GR, Cushman JC.** 2012. The *Vitis vinifera* C-repeat binding protein 4 (*VvCBF4*) transcriptional factor enhances freezing tolerance in wine grape. *Plant Biotechnology Journal* **10**, 105–124.
- Tuteja N, Gill SS, Tuteja R.** 2012. Improving crop productivity and abiotic stress tolerance in cultivated *Fragaria* using omics and systems biology approach. In: Rohloff J, Barah P, Bones AM, eds. *Improving crop productivity in sustainable agriculture*. Weinheim: Wiley VCH, 451–484.
- Vega-Alvarez M, Salazar-Salas NY, López-Angulo G, Pineda-Hidalgo KV, López-López ME, Vega-García MO, Delgado-Vargas F, López-Valenzuela JA.** 2020. Metabolomic changes in mango fruit peel associated with chilling injury tolerance induced by quarantine hot water treatment. *Postharvest Biology and Technology* **169**, 111299.
- Verbruggen N, Hermans C.** 2008. Proline accumulation in plants: a review. *Amino Acids* **35**, 753–759.

- Villarreal NM, Martínez GA, Civello PM.** 2009. Influence of plant growth regulators on polygalacturonase expression in strawberry fruit. *Plant Science* **176**, 749–757.
- Wang L, Nick P.** 2017. Cold sensing in grapevine—which signals are upstream of the microtubular ‘thermometer’. *Plant, Cell & Environment* **40**, 2844–2857.
- Wang L, Sadeghnejad E, Riemann M, Peter N.** 2019. Microtubule dynamics modulate sensing during cold acclimation in grapevine suspension cells. *Plant Science* **280**, 18–30.
- Wang L, Sadeghnezhad E, Nick P.** 2020. Upstream of gene expression: what is the role of microtubules in cold signalling? *Journal of Experimental Botany* **71**, 36–48.
- Wang L, Wang Y, Hou YY, Zhu X, Zheng YH, Jin P.** 2021. Physiological and metabolomic analyses of hot water treatment on amino acids and phenolic metabolisms in peach cold tolerance. *Postharvest Biology and Technology* **179**, 111593.
- Whitaker VM, Knapp SJ, Hardigan MA, et al.** 2020. A roadmap for research in octoploid strawberry. *Horticulture Research* **7**, 33.
- Xiao H, Tattersall EA, Siddiqua MK, Cramer GR, Nassuth A.** 2008. CBF4 is a unique member of the CBF transcription factor family of *Vitis vinifera* and *Vitis riparia*. *Plant, Cell & Environment* **31**, 1–10.
- Yen GC, Hsieh CL.** 1997. Antioxidant effects of dopamine and related compounds. *Bioscience, Biotechnology, and Biochemistry* **61**, 1646–1649.
- Yi X, Zhao B, Tang Y, Xu Z.** 2020. Transcriptome analysis reveals the regulation of metabolic processes during the post-harvest cold storage of pear. *Genomics* **112**, 3933–3942.
- Zhang B, Tieman DM, Jiao C, Xu Y, Chen K, Fei Z, Giovannoni JJ, Klee HJ.** 2016. Chilling-induced tomato flavor loss is associated with altered volatile synthesis and transient changes in DNA methylation. *Proceedings of the National Academy of Sciences, USA* **113**, 12580–12585.
- Zhao Y.** 2012. Auxin biosynthesis: a simple two-step pathway converts tryptophan to indole-3-acetic acid in plants. *Molecular Plant* **5**, 334–338.
- Zrenner R, Stitt M, Sonnewald U, Boldt R.** 2006. Pyrimidine and purine biosynthesis and degradation in plants. *Annual Review of Plant Biology* **57**, 805–836.